

A spectrally accurate method for the direct and inverse scattering problems by multiple 3D dielectric obstacles

Frédérique Le Louër¹

(Received 22 November 2016; revised 12 December 2017)

Abstract

We consider fast and accurate solution methods for the direct and inverse scattering problems by a few three dimensional piecewise homogeneous dielectric obstacles around the resonance region. The forward problem is reduced to a system of second kind boundary integral equations. For the numerical solution of these coupled integral equations we modify a fast and accurate spectral algorithm, proposed by Ganesh and Hawkins [doi:10.1016/j.jcp.2008.01.016], by transporting these equations onto the unit sphere using the Piola transform of the boundary parametrisations. The computational performances of the forward solver are demonstrated on numerical examples for a variety of three-dimensional smooth and non smooth obstacles. The algorithm, that requires the knowledge of the boundary parametrisation and leads

to invert small linear systems, is well-suited for the use of geometric optimisation tools to solve the inverse problem of recovering the shape of scatterers from the knowledge of noisy data. Computational details for the application of the iteratively regularised Gauss–Newton method to the numerical solution of the electromagnetic inverse problem are presented. Numerical experiments for the shape detection of multiple obstacles using incomplete radiation pattern data from back and front side are provided. The results in this article can also be applied for solving shape optimisation problems relying on time-harmonic electromagnetic waves.

Subject class: 45A05; 78A46; 78A40; 65N35; 65N21; 90C31

Keywords: Maxwell equations, multiple scattering, inverse problems, fast solver, Gauss–Newton method

Contents

1	Introduction	E3
2	The solution of the dielectric obstacle scattering problem	E8
3	Spherical reformulation of the boundary integral equations	E15
4	Fully discrete Galerkin method and examples	E19
5	Operator formulations and IRGN method	E24
6	The Fréchet derivative and its adjoint	E27
7	Implementation of the Newton method and numerical examples	E34
8	Conclusion	E39

1	<i>Introduction</i>	E3
A	Surface differential operators	E40
B	Spherical harmonics and Sobolev spaces on \mathbb{S}^2	E42
	References	E44

1 Introduction

The problem to reconstruct the shape of scatterers from noisy far-field or near-field measurements of time-harmonic waves arises in many fields of applied physics, for example sonar and radar applications, bio-medical imaging, non destructive testing or geophysical exploration. Such inverse problems are severely ill-posed. Often they are formulated as a nonlinear least squares problem, for which regularised iterative algorithm are applied to recover an approximate solution.

The numerical treatment of the inverse problem requires a fast and accurate solver for the forward problem. Here we consider the scattering of time-harmonic waves at a fixed frequency ω by three-dimensional bounded and non-conducting homogeneous dielectric obstacles represented by the domain Ω . The scatterers consist of $N \geq 1$ disjoint bounded obstacles Ω_ℓ with a smooth (of class \mathcal{C}^2 at least) closed simply connected boundary Γ_ℓ , and we have $\Omega = \bigcup_{\ell=1}^N \Omega_\ell$. The boundary of Ω is $\Gamma = \bigcup_{\ell=1}^N \Gamma_\ell$ where $\Gamma_\ell \cap \Gamma_{\ell'} = \emptyset$ if $\ell \neq \ell'$. The electric permittivity ε and the magnetic permeability μ are assumed to take constant values in the interior and in the exterior of the obstacles, but are discontinuous across the boundary Γ . The constant values of ε and μ may even be different inside each obstacles. The wavenumber is $\kappa = \omega\sqrt{\varepsilon\mu}$. In this case the forward problem is described by the system of Maxwell equations in the whole space \mathbb{R}^3 , with natural transmission conditions expressing the continuity of the tangential components of the magnetic and electric fields (\mathbf{H}, \mathbf{E}) across the boundary Γ . Let Ω^c denote the exterior domain $\mathbb{R}^3 \setminus \overline{\Omega}$ and \mathbf{n} denote the outer unit normal vector on the boundary Γ .

We label the dielectric quantities related to the interior domain Ω_ℓ by the index ℓ and to the exterior domain Ω^c by the index 0. For $\ell = 1, \dots, N$ we set $\mu_\ell = \mu|_{\Omega_\ell}$, $\kappa_\ell = \kappa|_{\Omega_\ell}$, and $\mathbf{n}_\ell = \mathbf{n}|_{\Gamma_\ell}$. Eliminating the magnetic field in the Maxwell system ($\mathbf{H} = 1/(\mathbf{i}\kappa) \mathbf{curl} \mathbf{E}$) we obtain the following transmission problem: Given an incident electric wave \mathbf{E}^{inc} which is assumed to solve the second order Maxwell equation in the absence of any dielectric scatterer, find the interior electric fields $\mathbf{E}^\ell = \mathbf{E}|_{\Omega_\ell}$ and the exterior scattered field $\mathbf{E}^s = \mathbf{E}|_{\Omega^c} - \mathbf{E}^{\text{inc}}$ that satisfies

$$\mathbf{curl} \mathbf{curl} \mathbf{E}^s - \kappa_0^2 \mathbf{E}^s = 0 \quad \text{in } \Omega^c, \quad (1a)$$

$$\mathbf{curl} \mathbf{curl} \mathbf{E}^\ell - \kappa_\ell^2 \mathbf{E}^\ell = 0 \quad \text{in } \Omega_\ell, \text{ for } \ell = 1, \dots, N, \quad (1b)$$

and the transmission conditions on Γ_ℓ ,

$$\mathbf{n}_\ell \times \mathbf{E}^\ell = \mathbf{n}_\ell \times (\mathbf{E}^s + \mathbf{E}^{\text{inc}}), \quad (1c)$$

$$\frac{1}{\mu_\ell} \mathbf{n}_\ell \times \mathbf{curl} \mathbf{E}^\ell = \frac{1}{\mu_0} \mathbf{n}_\ell \times \mathbf{curl} (\mathbf{E}^s + \mathbf{E}^{\text{inc}}). \quad (1d)$$

In addition the scattered field \mathbf{E}^s has to satisfy the Silver–Müller radiation condition

$$\lim_{|\mathbf{x}| \rightarrow +\infty} |\mathbf{x}| \left| \mathbf{curl} \mathbf{E}^s(\mathbf{x}) \times \frac{\mathbf{x}}{|\mathbf{x}|} - \mathbf{i}\omega\mu_0 \mathbf{E}^s(\mathbf{x}) \right| = 0. \quad (1e)$$

uniformly in all directions $\mathbf{x}/|\mathbf{x}|$.

Well-posedness of the dielectric obstacle scattering problem for any positive real values of the dielectric constants is well known, and this problem can be reduced in several different ways to coupled or single boundary integral equations on the dielectric interface Γ : Harrington [23] and Martin and Ola [40] overviewed these formulations for a single simply connected smooth boundary. Some pairs of integral equations have irregular frequencies and others do not, as the so-called Müller’s system [42]. Mautz [41] suggested that the use of single combined-field integral equation method avoids the occurrence of irregular frequencies. Existence of the solution was then proved by Ola and Martin via a regularisation technique. For a Lipschitz boundary, Buffa, Hiptmair, von Petersdorff and Schwab [4] derived a uniquely solvable system

of integral equations and Costabel and Le Louër [8, 36] constructed a family of four alternative single boundary integral equations extending a technique due to Kleinman and Martin [33] in acoustic scattering. All these formulations naturally extend to multiple obstacles and we focus here on Muller's system, namely the direct method, and its adjoint form, namely the indirect method. These dielectric integral equations suffer from low-frequency break down. Ganesh et al. [19] gave an all-frequency integral equation reformulation.

The radiation condition implies that the scattered field \mathbf{E}^s has an asymptotic behaviour of the form [7, Theorem 6.8]

$$\mathbf{E}^s(\mathbf{x}) = \frac{e^{i\kappa_0|\mathbf{x}|}}{|\mathbf{x}|} \left\{ \mathbf{E}^\infty(\hat{\mathbf{x}}) + O\left(\frac{1}{|\mathbf{x}|}\right) \right\}, \quad |\mathbf{x}| \rightarrow \infty,$$

uniformly in all directions $\hat{\mathbf{x}} = \mathbf{x}/|\mathbf{x}|$. The far-field pattern \mathbf{E}^∞ is a tangential vector function defined on the unit sphere \mathbb{S}^2 of \mathbb{R}^3 and is always analytic.

The forward problem discussed in this paper is the scattering of m incident plane waves of the form $\mathbf{E}_j^{\text{inc}}(\mathbf{x}) = \mathbf{p}_j e^{i\kappa_0 \mathbf{x} \cdot \mathbf{d}_j}$, $j = 1, \dots, m$, where $\mathbf{d}_j, \mathbf{p}_j \in \mathbb{S}^2$ and $\mathbf{d}_j \cdot \mathbf{p}_j = 0$. We denote by F_j the boundary to far-field operator that maps a parametrisation of the boundary Γ onto the far-field pattern \mathbf{E}_j^∞ of the scattered field \mathbf{E}_j^s of the solution $((\mathbf{E}_j^\ell)_{1 \leq \ell \leq N}, \mathbf{E}_j^s)$ to the problem (1a)–(1e) for the incident wave $\mathbf{E}_j^{\text{inc}}$. For simplicity we do not distinguish between the boundary Γ and its parametrisation in this introduction. The inverse problem consists in reconstructing Γ given noisy measured data described by

$$\mathbf{E}_{j,\delta}^\infty = F_j(\Gamma) + \text{err}_j, \quad j = 1, \dots, m, \quad \sum_{j=1}^m \|\text{err}_j\|^2 \leq \delta^2. \quad (2)$$

Here measurement errors are described by the functions err_j , and the error bound δ , the incident fields $\mathbf{E}_j^{\text{inc}}$, and the dielectric constants are assumed to be known. In practice, equation (2) is posed on a subset Γ_{obs} of the far-field sphere \mathbb{S}^2 . By straightforward modifications of the algorithm described in Section 5, one could simultaneously invert for Γ and the dielectric constants [1,

Section 3.2]. In this situation Hähner [21] showed a uniqueness result assuming knowledge of the far-field patterns for all incoming plane waves. However, even with known dielectric constants it remains an open question whether or not Γ is uniquely determined by only a finite number of incoming plane waves.

Over the last two decades, much attention has been devoted to the investigation of efficient iterative methods, in particular regularised Newton-type method for nonlinear ill-posed problems via first order linearisation [3, 27, 28, 32]. Until now, it was successfully applied to inverse acoustic scattering problems [22, 28]. Indeed, the use of such iterative methods requires the analysis and an explicit form of the Fréchet derivatives of the boundary to far-field operators F_j . The Fréchet derivative of the far-field pattern is usually interpreted as the far-field pattern of a new scattering problem and these characterisations are well-known in acoustic scattering since the 1990s. Many different approaches were used: Fréchet differentiability of the far-field (or of the solution away from the boundary) was established by Kirsch [32] and Hettlich [24, 25] via variational methods, by Potthast via boundary integral representations [45, 47], by Hohage [28] and Schormann [29] via the implicit function theorem, and by Kress and Päiväranta via Green's theorem and a far-field identity [35].

In electromagnetism, Fréchet differentiability was first investigated by Potthast [46] for the perfect conductor problem extending the boundary integral equation approach. The characterisation of the derivative was then improved by Kress [34]. More recently, Fréchet differentiability was analyzed by Haddar and Kress [20] for the Neumann-impedance type obstacle scattering problem via the use of a far-field identity and by Costabel and Le Louër [9, 10, 36] and Hettlich [26] for the dielectric scattering problem via the boundary integral equation approach [8, 36] and variational methods, respectively.

This paper applies the iteratively regularised Gauss–Newton (IRGN) method, combined with a fast forward solver, to solve the inverse scattering problem for multiple dielectric obstacles. Section 2 describes the two different bound-

ary integral equation methods that are used to solve the electromagnetic transmission problem via direct and indirect approaches. [Section 3](#) proposes a new spectral method to solve these systems which ensures super-algebraic convergence of the discrete solution to the exact solution, in the case of multiple simply connected closed surfaces. The idea of the method originates from Atkinson's work [2], where he suggested a Galerkin method for the Laplace equation using spherical harmonics as basis functions. Many advances on that subject led to the high-order algorithm proposed by Ganesh and Graham [12] for the Helmholtz equation and to the one proposed by Ganesh and Hawkins [16] for the Maxwell equations, in the context of the perfect conductor problem. They proposed first two methods by transporting the boundary integral equation on the unit sphere using a change of variable and then by looking for a solution in terms of series (component-wise) of scalar spherical harmonics [13] or of series of vector spherical harmonics [14, 15]. To decrease the number of unknowns, they introduce a normal transformation acting from the tangent plane to the boundary Γ onto the tangent plane to the unit sphere, so that one only has to seek a solution in terms of tangential vector spherical harmonics [16]. The latter approach was extended to the solution of the scattering problem by multiple perfect conductors [17]. Here we use a different approach based on the Piola transform of a diffeomorphism from \mathbb{S}^2 to Γ that maps the energy space $\mathbf{H}_{\text{div}}^{-1/2}(\Gamma)$, defined in [Section 2](#), onto the space $\mathbf{H}_{\text{div}}^{-1/2}(\mathbb{S}^2)$. The numerical implementation is briefly described in [Section 4](#) and numerical results on the convergence rate of the method are presented for smooth and non smooth obstacles. The mathematical analysis renders even possible the implementation of hypersingular kernels [37, 38]. However, in the extreme low-frequency regime, as $\omega \rightarrow 0$, numerical methods that use only tangential basis functions are not sufficient to avoid the low-frequency breakdown [19].

In [Section 5](#) we recall the main results on the Fréchet differentiability of the boundary to far-field operator and give a characterisation of the adjoint operator which is needed in the implementation of the regularised Newton method. [Section 6](#) presents the inverse scattering algorithm in the special case

of star-shaped obstacles that are also described by spherical harmonics. The properties of the Piola transform allows analytical numerical evaluation of boundary data characterising the Fréchet derivatives. The forward algorithm consists of many nested loops, so the running speed of the whole inverse algorithm is improved using parallel computations. Numerical experiments are presented in [Section 7](#). Finally, [Section 8](#) concludes with some remarks and possible research lines.

2 The solution of the dielectric obstacle scattering problem

We denote by $\mathbf{H}^s(\Omega)$, $\mathbf{H}_{\text{loc}}^s(\overline{\Omega^c})$ and $\mathbf{H}^s(\Gamma)$ the standard (local in the case of the exterior domain) complex valued, Hilbertian Sobolev space of order $s \in \mathbb{R}$ defined on Ω , $\overline{\Omega^c}$ and Γ respectively (with the convention $\mathbf{H}^0 = \mathbf{L}^2$.) Spaces of vector functions are denoted by boldface letters, thus $\mathbf{H}^s = (\mathbf{H}^s)^3$. Moreover, $\mathbf{H}_t^s(\Gamma) := \{\boldsymbol{\varphi} \in \mathbf{H}^s(\Gamma) : \boldsymbol{\varphi} \cdot \mathbf{n} = 0\}$ denotes the Sobolev space of tangential vector fields of order $s \in \mathbb{R}$. For a differential operator Λ we set

$$\begin{aligned} \mathbf{H}(\Lambda, \Omega) &= \{\mathbf{v} \in \mathbf{L}^2(\Omega) : \Lambda \mathbf{v} \in \mathbf{L}^2(\Omega)\}, \\ \mathbf{H}_{\text{loc}}(\Lambda, \Omega^c) &= \{\mathbf{v} \in \mathbf{L}_{\text{loc}}^2(\overline{\Omega^c}) : \Lambda \mathbf{v} \in \mathbf{L}_{\text{loc}}^2(\overline{\Omega^c})\}. \end{aligned}$$

The space $\mathbf{H}(\Lambda, \Omega)$ is endowed with the natural graph norm $\|\mathbf{v}\|_{\mathbf{H}(\Lambda, \Omega)}^2 := \|\mathbf{v}\|_{\mathbf{L}^2(\Omega)}^2 + \|\Lambda \mathbf{v}\|_{\mathbf{L}^2(\Omega)}^2$. This defines in particular the Hilbert spaces $\mathbf{H}(\mathbf{curl}, \Omega)$ and $\mathbf{H}(\mathbf{curl curl}, \Omega)$ and Fréchet spaces $\mathbf{H}_{\text{loc}}(\mathbf{curl}, \Omega^c)$ and $\mathbf{H}_{\text{loc}}(\mathbf{curl curl}, \Omega^c)$. Analogously, we introduce the Hilbert space

$$\mathbf{H}_{\text{div}}^{-1/2}(\Gamma) = \left\{ \boldsymbol{\varphi} \in \mathbf{H}_t^{-1/2}(\Gamma) : \text{div}_{\Gamma} \boldsymbol{\varphi} \in \mathbf{H}^{-1/2}(\Gamma) \right\}$$

endowed with the norm $\|\cdot\|_{\mathbf{H}_{\text{div}}^{-1/2}(\Gamma)} = (\|\cdot\|_{\mathbf{H}^{-1/2}(\Gamma)}^2 + \|\text{div}_{\Gamma} \cdot\|_{\mathbf{H}^{-1/2}(\Gamma)}^2)^{1/2}$. We have

$$\boldsymbol{\varphi} \in \mathbf{H}_{\text{div}}^{-1/2}(\Gamma) \Leftrightarrow \text{for all } \ell = 1, \dots, N, \quad \boldsymbol{\varphi}_{\ell} = \boldsymbol{\varphi}|_{\Gamma_{\ell}} \in \mathbf{H}_{\text{div}}^{-1/2}(\Gamma_{\ell}).$$

Recall that for a vector function $\mathbf{u} \in \mathbf{H}(\mathbf{curl}, \Omega) \cap \mathbf{H}(\mathbf{curl curl}, \Omega)$, the traces $\mathbf{n} \times \mathbf{u}|_{\Gamma}$ and $\mathbf{n} \times \mathbf{curl} \mathbf{u}|_{\Gamma}$ are in $\mathbf{H}_{\text{div}}^{-1/2}(\Gamma)$ [43, e.g.].

Let $\Phi(\kappa, \mathbf{x}) = \frac{e^{i\kappa|\mathbf{x}|}}{4\pi|\mathbf{x}|}$ denote the fundamental solution of the Helmholtz equation $\Delta \mathbf{u} + \kappa^2 \mathbf{u} = 0$. Any radiating solution \mathbf{E}^s to the Maxwell equation (1a)–(1e) in Ω^c satisfies the Stratton–Chu representation formula

$$\mathbf{E}^s = \sum_{\ell=1}^N \left[\mathcal{M}_{\kappa_0}^{\ell} \left(\mathbf{n}_{\ell} \times \mathbf{E}_{|\Gamma_{\ell}}^s \right) + \frac{\mu_0}{\kappa_0} \mathcal{C}_{\kappa_0}^{\ell} \left(\frac{1}{\mu_0} \mathbf{n}_{\ell} \times (\mathbf{curl} \mathbf{E}^s)_{|\Gamma_{\ell}} \right) \right] \Big|_{\Omega^c}, \quad (3)$$

where $\mathcal{C}_{\kappa}^{\ell}$ and $\mathcal{M}_{\kappa}^{\ell}$ are, respectively, the single and double layer potential operators defined for any tangential density $\boldsymbol{\varphi} \in \mathbf{H}_{\text{div}}^{-1/2}(\Gamma_{\ell})$ and $\mathbf{x} \in \mathbb{R}^3 \setminus \Gamma_{\ell}$ by

$$\begin{aligned} (\mathcal{C}_{\kappa}^{\ell} \boldsymbol{\varphi})(\mathbf{x}) &= \frac{1}{\kappa} \int_{\Gamma_{\ell}} \mathbf{curl} \mathbf{curl}^{\mathbf{x}} \{ \Phi(\kappa, \mathbf{x} - \mathbf{y}) \boldsymbol{\varphi}(\mathbf{y}) \} d\sigma(\mathbf{y}), \\ (\mathcal{M}_{\kappa}^{\ell} \boldsymbol{\varphi})(\mathbf{x}) &= \int_{\Gamma_{\ell}} \mathbf{curl}^{\mathbf{x}} \{ \Phi(\kappa, \mathbf{x} - \mathbf{y}) \boldsymbol{\varphi}(\mathbf{y}) \} d\sigma(\mathbf{y}). \end{aligned}$$

By Green’s second formula in Ω , for $\mathbf{x} \in \Omega^c$,

$$\mathbf{0} = \sum_{\ell=1}^N \left[\mathcal{M}_{\kappa_0}^{\ell} \left(\mathbf{n}_{\ell} \times \mathbf{E}_{|\Gamma_{\ell}}^{\text{inc}} \right) + \frac{\mu_0}{\kappa_0} \mathcal{C}_{\kappa_0}^{\ell} \left(\frac{1}{\mu_0} \mathbf{n}_{\ell} \times (\mathbf{curl} \mathbf{E}^{\text{inc}})_{|\Gamma_{\ell}} \right) \right] \Big|_{\Omega^c}(\mathbf{x}). \quad (4)$$

Adding (3) and (4) we obtain the following integral representation for the scattered wave

$$\begin{aligned} \mathbf{E}^s &= \sum_{\ell=1}^N \left[\mathcal{M}_{\kappa_0}^{\ell} \left(\mathbf{n}_{\ell} \times (\mathbf{E}^s + \mathbf{E}^{\text{inc}})_{|\Gamma_{\ell}} \right) \right. \\ &\quad \left. + \frac{\mu_0}{\kappa_0} \mathcal{C}_{\kappa_0}^{\ell} \left(\frac{1}{\mu_0} \mathbf{n}_{\ell} \times (\mathbf{curl} \mathbf{E}^s + \mathbf{curl} \mathbf{E}^{\text{inc}})_{|\Gamma_{\ell}} \right) \right] \Big|_{\Omega^c}. \quad (5) \end{aligned}$$

Analogously, for solutions \mathbf{E}^{ℓ} to Maxwell’s equations (1b) in the interior domain Ω_{ℓ} , for $\ell = 1, \dots, N$, the Stratton–Chu representation formula reads

$$\mathbf{E}_{|\Omega_{\ell}}^{\ell} = - \left[\frac{\mu_{\ell}}{\kappa_{\ell}} \mathcal{C}_{\kappa_{\ell}}^{\ell} \left(\frac{1}{\mu_{\ell}} \mathbf{n}_{\ell} \times (\mathbf{curl} \mathbf{E}^{\ell})_{|\Gamma_{\ell}} \right) + \mathcal{M}_{\kappa_{\ell}}^{\ell} \left(\mathbf{n}_{\ell} \times \mathbf{E}_{|\Gamma_{\ell}}^{\ell} \right) \right] \Big|_{\Omega_{\ell}}, \quad (6)$$

and the Green's second formula in Ω_ℓ , for $\ell = 1, \dots, N$, gives

$$\mathbf{0} = - \left[\frac{\mu_\ell}{\kappa_\ell} \mathbf{C}_{\kappa_\ell}^\ell \left(\frac{1}{\mu_\ell} \mathbf{n}_\ell \times (\mathbf{curl} \mathbf{E}^\ell)_{|\Gamma_\ell} \right) + \mathcal{M}_{\kappa_\ell}^\ell \left(\mathbf{n}_\ell \times \mathbf{E}_{|\Gamma_\ell}^\ell \right) \right] (\mathbf{x}), \quad \mathbf{x} \in \mathbb{R}^3 \setminus \overline{\Omega_\ell}. \quad (7)$$

By (5) and (6), one can see that the solution of the forward problem is uniquely determined by the knowledge of the interior boundary values $\mathbf{n}_\ell \times \mathbf{E}_{|\Gamma_\ell}^\ell$ and $\frac{1}{\mu_\ell} \mathbf{n}_\ell \times (\mathbf{curl} \mathbf{E}^\ell)_{|\Gamma_\ell}$ and the exterior boundary values $\mathbf{n}_\ell \times (\mathbf{E}^s + \mathbf{E}^{\text{inc}})_{|\Gamma_\ell}$ and $\frac{1}{\mu_0} \mathbf{n}_\ell \times \mathbf{curl}(\mathbf{E}^s + \mathbf{E}^{\text{inc}})_{|\Gamma_\ell}$, for $\ell = 1, \dots, N$. Thanks to the transmission conditions (1c) one can reduce in several different ways the dielectric scattering problem to a system of N coupled equations posed on Γ_ℓ . The most attractive boundary integral formulation of the problem via a direct method is Müller's [42] since it yields a uniquely solvable system of boundary integral equations of the second kind for all positive values of the dielectric constants. Direct methods has the additional advantage to provide the physical boundary data of the total field solution.

To derive the boundary integral formulation we introduce the single layer potential \mathbf{C}_κ^ℓ and the double layer potential \mathbf{M}_κ^ℓ in electromagnetic potential theory defined by

$$\begin{aligned} (\mathbf{C}_\kappa^\ell \boldsymbol{\varphi})(\mathbf{x}) &= \frac{1}{\kappa} \int_{\Gamma_\ell} \mathbf{n}_\ell(\mathbf{x}) \times \mathbf{curl}^{\mathbf{x}} \mathbf{curl}^{\mathbf{x}} \{2\Phi(\kappa, \mathbf{x} - \mathbf{y}) \boldsymbol{\varphi}(\mathbf{y})\} \mathbf{ds}(\mathbf{y}), \\ (\mathbf{M}_\kappa^\ell \boldsymbol{\varphi})(\mathbf{x}) &= \int_{\Gamma_\ell} \mathbf{n}_\ell(\mathbf{x}) \times \mathbf{curl}^{\mathbf{x}} \{2\Phi(\kappa, \mathbf{x} - \mathbf{y}) \boldsymbol{\varphi}(\mathbf{y})\} \mathbf{ds}(\mathbf{y}). \end{aligned}$$

(The factor 2 in the definition of \mathbf{C}_κ^ℓ and \mathbf{M}_κ^ℓ avoids the occurrence of a factor $\frac{1}{2}$ in the Calderón formula and then in the boundary integral equations system.) The operator $\mathbf{M}_\kappa^\ell : \mathbf{H}_{\text{div}}^{-1/2}(\Gamma_\ell) \rightarrow \mathbf{H}_{\text{div}}^{-1/2}(\Gamma_\ell)$ is compact and the operator \mathbf{C}_κ^ℓ is of order +1 but bounded on $\mathbf{H}_{\text{div}}^{-1/2}(\Gamma_\ell)$. The Calderón projectors for the time-harmonic Maxwell equation (1b) are $\mathbf{P}_\ell = \mathbf{I} - \mathbf{A}_\ell$ and $\mathbf{P}_\ell^c = \mathbf{I} + \mathbf{A}_\ell$ where

$$\mathbf{A}_\ell = \begin{bmatrix} \mathbf{M}_{\kappa_\ell}^\ell & \mathbf{C}_{\kappa_\ell}^\ell \\ \mathbf{C}_{\kappa_\ell}^\ell & \mathbf{M}_{\kappa_\ell}^\ell \end{bmatrix}.$$

From (6) and (7) we deduce

$$\mathbf{P}_\ell \begin{bmatrix} \mathbf{n}_\ell \times \mathbf{E}_{|\Gamma_\ell}^\ell \\ \frac{1}{\kappa_\ell} \mathbf{n}_\ell \times \mathbf{curl} \mathbf{E}_{|\Gamma_\ell}^\ell \end{bmatrix} = \begin{bmatrix} 2\mathbf{n}_\ell \times \mathbf{E}_{|\Gamma_\ell}^\ell \\ \frac{2}{\kappa_\ell} \mathbf{n}_\ell \times \mathbf{curl} \mathbf{E}_{|\Gamma_\ell}^\ell \end{bmatrix}, \quad \mathbf{P}_\ell^c \begin{bmatrix} \mathbf{n}_\ell \times \mathbf{E}_{|\Gamma_\ell}^\ell \\ \frac{1}{\kappa_\ell} \mathbf{n}_\ell \times \mathbf{curl} \mathbf{E}_{|\Gamma_\ell}^\ell \end{bmatrix} = \mathbf{0}. \quad (8)$$

The Calderón projectors, on the boundary Γ_ℓ , for the time-harmonic Maxwell equation (1a) are defined for any densities $\boldsymbol{\varphi} := (\boldsymbol{\varphi}_\ell)_{1 \leq \ell \leq N} \in \mathbf{H}_{\text{div}}^{-1/2}(\Gamma)$ and $\boldsymbol{\psi} := (\boldsymbol{\psi}_\ell)_{1 \leq \ell \leq N} \in \mathbf{H}_{\text{div}}^{-1/2}(\Gamma)$ by

$$\begin{aligned} \mathbf{P}_{0,\ell} \begin{bmatrix} \boldsymbol{\varphi} \\ \boldsymbol{\psi} \end{bmatrix} &= (\mathbf{I} - \mathcal{A}_0^\ell) \begin{bmatrix} \boldsymbol{\varphi}_\ell \\ \boldsymbol{\psi}_\ell \end{bmatrix} - \sum_{\ell' \neq \ell} \mathcal{A}_0^{\ell,\ell'} \begin{bmatrix} \boldsymbol{\varphi}_{\ell'} \\ \boldsymbol{\psi}_{\ell'} \end{bmatrix}, \\ \mathbf{P}_{0,\ell}^c \begin{bmatrix} \boldsymbol{\varphi} \\ \boldsymbol{\psi} \end{bmatrix} &= (\mathbf{I} + \mathcal{A}_0^\ell) \begin{bmatrix} \boldsymbol{\varphi}_\ell \\ \boldsymbol{\psi}_\ell \end{bmatrix} + \sum_{\ell' \neq \ell} \mathcal{A}_0^{\ell,\ell'} \begin{bmatrix} \boldsymbol{\varphi}_{\ell'} \\ \boldsymbol{\psi}_{\ell'} \end{bmatrix}, \end{aligned}$$

where \mathcal{A}_0^ℓ and $\mathcal{A}_0^{\ell,\ell'}$ are defined by

$$\mathcal{A}_0^\ell = \begin{bmatrix} \mathcal{M}_{\kappa_0}^\ell & \mathcal{C}_{\kappa_0}^\ell \\ \mathcal{C}_{\kappa_0}^{\ell'} & \mathcal{M}_{\kappa_0}^{\ell'} \end{bmatrix} \quad \text{and} \quad \mathcal{A}_0^{\ell,\ell'} = \begin{bmatrix} 2\mathbf{R}_\ell & 0 \\ 0 & 2\mathbf{R}_\ell \end{bmatrix} \begin{bmatrix} \mathcal{M}_{\kappa_0}^{\ell'} & \mathcal{C}_{\kappa_0}^{\ell'} \\ \mathcal{C}_{\kappa_0}^{\ell'} & \mathcal{M}_{\kappa_0}^{\ell'} \end{bmatrix},$$

and \mathbf{R}_ℓ is the operator defined by $\mathbf{R}_\ell \mathbf{E} = \mathbf{n}_\ell \times \mathbf{E}_{|\Gamma_\ell}$. Then, from (5) we deduce

$$\mathbf{P}_{0,\ell} \begin{bmatrix} \mathbf{n} \times (\mathbf{E}^s + \mathbf{E}^{\text{inc}})_{|\Gamma} \\ \frac{1}{\kappa_0} \mathbf{n} \times \mathbf{curl} (\mathbf{E}^s + \mathbf{E}^{\text{inc}})_{|\Gamma} \end{bmatrix} = \begin{bmatrix} 2\mathbf{n}_\ell \times \mathbf{E}_{|\Gamma_\ell}^{\text{inc}} \\ \frac{2}{\kappa_0} \mathbf{n}_\ell \times \mathbf{curl} \mathbf{E}_{|\Gamma_\ell}^{\text{inc}} \end{bmatrix}. \quad (9)$$

Now we set

$$\begin{aligned} \mathbf{u}_\ell^s &= \begin{bmatrix} \mathbf{n}_\ell \times \mathbf{E}_{|\Gamma_\ell}^s \\ \frac{1}{\mu_0} \mathbf{n}_\ell \times \mathbf{curl} \mathbf{E}_{|\Gamma_\ell}^s \end{bmatrix}, \quad \mathbf{u}_\ell^{\text{inc}} = \begin{bmatrix} \mathbf{n}_\ell \times \mathbf{E}_{|\Gamma_\ell}^{\text{inc}} \\ \frac{1}{\mu_0} \mathbf{n}_\ell \times \mathbf{curl} \mathbf{E}_{|\Gamma_\ell}^{\text{inc}} \end{bmatrix}, \\ \mathbf{u}_\ell^i &= \begin{bmatrix} \mathbf{n}_\ell \times \mathbf{E}_{|\Gamma_\ell}^\ell \\ \frac{1}{\mu_\ell} \mathbf{n}_\ell \times \mathbf{curl} \mathbf{E}_{|\Gamma_\ell}^\ell \end{bmatrix}. \end{aligned}$$

By virtue of (8) and (9) for $\ell = 1, \dots, N$

$$\mathbf{0} = \begin{bmatrix} \frac{\mu_0 \kappa_\ell^2}{\mu_\ell \kappa_0^2} & 0 \\ 0 & \frac{\kappa_\ell}{\mu_0} \end{bmatrix} \mathbf{P}_\ell^c \begin{bmatrix} 1 & 0 \\ 0 & \frac{\mu_\ell}{\kappa_\ell} \end{bmatrix} \mathbf{u}_\ell^i, \quad (10)$$

$$2\mathbf{u}_\ell^{\text{inc}} = \begin{bmatrix} 1 & 0 \\ 0 & \frac{\kappa_0}{\mu_0} \end{bmatrix} \mathbf{P}_{0,\ell} \begin{bmatrix} 1 & 0 \\ 0 & \frac{\mu_0}{\kappa_0} \end{bmatrix} (\mathbf{u}^s + \mathbf{u}^{\text{inc}}), \quad (11)$$

and the transmission conditions give

$$\mathbf{u}_\ell^i = \mathbf{u}_\ell^s + \mathbf{u}_\ell^{\text{inc}}. \quad (12)$$

Müller's boundary integral formulation has to be solved for the unknowns $\mathbf{u}_\ell^s + \mathbf{u}_\ell^{\text{inc}}$ and is obtained by substituting (12) into (10) and combining the equalities (10) and (11) for $\ell = 1, \dots, N$ as follows:

$$\begin{bmatrix} \left(1 + \frac{\mu_0 \kappa_\ell^2}{\mu_\ell \kappa_0^2}\right) \mathbf{I} - \left(\mathbf{M}_{\kappa_0}^\ell - \frac{\mu_0 \kappa_\ell^2}{\mu_\ell \kappa_0^2} \mathbf{M}_{\kappa_\ell}^\ell\right) & -\frac{\mu_0}{\kappa_0^2} (\kappa_0 \mathbf{C}_{\kappa_0}^\ell - \kappa_\ell \mathbf{C}_{\kappa_\ell}^\ell) \\ -\frac{1}{\mu_0} (\kappa_0 \mathbf{C}_{\kappa_0}^\ell - \kappa_\ell \mathbf{C}_{\kappa_\ell}^\ell) & \left(1 + \frac{\mu_\ell}{\mu_0}\right) \mathbf{I} - \left(\mathbf{M}_{\kappa_0}^\ell - \frac{\mu_\ell}{\mu_0} \mathbf{M}_{\kappa_\ell}^\ell\right) \end{bmatrix} \cdot (\mathbf{u}_\ell^s + \mathbf{u}_\ell^{\text{inc}}) - 2 \sum_{\ell' \neq \ell} \begin{bmatrix} \mathbf{R}_\ell \mathcal{M}_{\kappa_0}^{\ell'} & \frac{\mu_0}{\kappa_0} \mathbf{R}_\ell \mathcal{C}_{\kappa_0}^{\ell'} \\ \frac{\kappa_0}{\mu_0} \mathbf{R}_\ell \mathcal{C}_{\kappa_0}^{\ell'} & \mathbf{R}_\ell \mathcal{M}_{\kappa_0}^{\ell'} \end{bmatrix} (\mathbf{u}_{\ell'}^s + \mathbf{u}_{\ell'}^{\text{inc}}) = 2\mathbf{u}_\ell^{\text{inc}}. \quad (13)$$

Since $\kappa_\ell \mathbf{C}_{\kappa_\ell}^\ell - \kappa_0 \mathbf{C}_{\kappa_0}^\ell$ is compact on $\mathbf{H}_t^{-1/2}(\Gamma_\ell)$ for $\ell = 1, \dots, N$, the integral operator associated to the system of N coupled equations (13) is a Fredholm operator of the second kind on the Hilbert space $\mathbf{H}_t^{-1/2}(\Gamma)$. The condition $\mathbf{u}_\ell^{\text{inc}} \in (\mathbf{H}_{\text{div}}^{-1/2}(\Gamma_\ell))^2$ guarantees that the solution to the integral equation is in $(\mathbf{H}_{\text{div}}^{-1/2}(\Gamma))^2$ too.

We present now an alternative approach via an indirect method in order to derive another second kind system of integral equations [40]. Indirect methods are used to solve electromagnetic transmission problem with general transmission conditions on Γ_ℓ of the form

$$\begin{aligned} \mathbf{n}_\ell \times \mathbf{E}_{|\Gamma_\ell}^s - \mathbf{n}_\ell \times \mathbf{E}_{|\Gamma_\ell}^\ell &= \mathbf{f}_\ell, \\ \frac{1}{\mu_0} \mathbf{n}_\ell \times \mathbf{curl} \mathbf{E}_{|\Gamma_\ell}^s - \frac{1}{\mu_\ell} \mathbf{n} \times \mathbf{curl} \mathbf{E}_{|\Gamma_\ell}^\ell &= \mathbf{g}_\ell, \end{aligned} \quad (14)$$

where the given boundary data $\mathbf{f}_\ell, \mathbf{g}_\ell \in \mathbf{H}_{\text{div}}^{-1/2}(\Gamma_\ell)$ are non physical quantities as in the characterisation of the Fréchet derivatives (28). In our case the indirect approach is based on the layer ansatz

$$\mathbf{E}^s = \sum_{\ell=1}^N \left[\mathcal{M}_{\kappa_0}^\ell \boldsymbol{\varphi}_\ell^s + \frac{\mu_0}{\kappa_0} \mathcal{C}_{\kappa_0}^\ell \boldsymbol{\psi}_\ell^s \right] \Big|_{\Omega^c} \quad \text{and} \quad \mathbf{E}_{|\Omega_\ell}^\ell = \left[\mathcal{M}_{\kappa_\ell}^\ell \boldsymbol{\varphi}_\ell^i + \frac{\mu_\ell}{\kappa_\ell} \mathcal{C}_{\kappa_\ell}^\ell \boldsymbol{\psi}_\ell^i \right] \Big|_{\Omega_\ell}, \quad (15)$$

where for $\ell = 1, \dots, N$, $\boldsymbol{\varphi}_\ell^s, \boldsymbol{\psi}_\ell^s, \boldsymbol{\varphi}_\ell^i, \boldsymbol{\psi}_\ell^i$ are tangential densities in $\mathbf{H}_{\text{div}}^{-1/2}(\Gamma_\ell)$. By virtue of (3) and (6) and the jump relations of the electromagnetic potentials

$$\mathbb{P}_\ell \begin{bmatrix} \boldsymbol{\varphi}_\ell^i \\ \frac{\mu_\ell}{\kappa_\ell} \boldsymbol{\psi}_\ell^i \end{bmatrix} = \begin{bmatrix} -2 \mathbf{n}_\ell \times \mathbf{E}_{|\Gamma_\ell}^\ell \\ -\frac{2}{\kappa_\ell} \mathbf{n}_\ell \times \mathbf{curl} \mathbf{E}_{|\Gamma_\ell}^\ell \end{bmatrix} \quad \text{and} \quad \mathbb{P}_{0,\ell}^c \begin{bmatrix} \boldsymbol{\varphi}^s \\ \frac{\mu_0}{\kappa_0} \boldsymbol{\psi}^s \end{bmatrix} = \begin{bmatrix} 2 \mathbf{n}_\ell \times \mathbf{E}_{|\Gamma_\ell}^s \\ \frac{2}{\kappa_0} \mathbf{n}_\ell \times \mathbf{curl} \mathbf{E}_{|\Gamma_\ell}^s \end{bmatrix}.$$

The transmission conditions yields

$$\begin{bmatrix} 1 & 0 \\ 0 & \frac{\kappa_\ell}{\mu_\ell} \end{bmatrix} \mathbb{P}_\ell \begin{bmatrix} \boldsymbol{\varphi}_\ell^i \\ \frac{\mu_\ell}{\kappa_\ell} \boldsymbol{\psi}_\ell^i \end{bmatrix} + \begin{bmatrix} 1 & 0 \\ 0 & \frac{\kappa_0}{\mu_0} \end{bmatrix} \mathbb{P}_{0,\ell}^c \begin{bmatrix} \boldsymbol{\varphi}^s \\ \frac{\mu_0}{\kappa_0} \boldsymbol{\psi}^s \end{bmatrix} = 2 \begin{bmatrix} \mathbf{f}_\ell \\ \mathbf{g}_\ell \end{bmatrix}.$$

We set $\boldsymbol{\varphi}_\ell^i = \frac{\mu_\ell}{\mu_0} \boldsymbol{\varphi}_\ell$, $\boldsymbol{\varphi}_\ell^s = \boldsymbol{\varphi}_\ell$ and $\boldsymbol{\psi}_\ell^i = \frac{\mu_0 \kappa_\ell^2}{\mu_\ell \kappa_0^2} \boldsymbol{\psi}_\ell$, $\boldsymbol{\psi}_\ell^s = \boldsymbol{\psi}_\ell$. Then we arrive at the following system of integral equations first obtained by Ola and Martin [40] for the single scattering problem:

$$\begin{aligned} & \left[\begin{array}{cc} \left(1 + \frac{\mu_0 \kappa_0^2}{\mu_\ell \kappa_\ell^2}\right) \mathbf{I} + \left(\mathcal{M}_{\kappa_0}^\ell - \frac{\mu_0 \kappa_0^2}{\mu_\ell \kappa_\ell^2} \mathcal{M}_{\kappa_\ell}^\ell\right) & \frac{1}{\mu_0} (\kappa_0 \mathcal{C}_{\kappa_0}^\ell - \kappa_\ell \mathcal{C}_{\kappa_\ell}^\ell) \\ \frac{\mu_0}{\kappa_0^2} (\kappa_0 \mathcal{C}_{\kappa_0}^\ell - \kappa_\ell \mathcal{C}_{\kappa_\ell}^\ell) & \left(1 + \frac{\mu_\ell}{\mu_0}\right) \mathbf{I} + \left(\mathcal{M}_{\kappa_0}^\ell - \frac{\mu_\ell}{\mu_0} \mathcal{M}_{\kappa_\ell}^\ell\right) \end{array} \right] \begin{bmatrix} \boldsymbol{\psi}_\ell \\ \boldsymbol{\varphi}_\ell \end{bmatrix} \\ & + 2 \sum_{\ell' \neq \ell} \begin{bmatrix} \mathbf{R}_\ell \mathcal{M}_{\kappa_0}^{\ell'} & \frac{\kappa_0}{\mu_0} \mathbf{R}_\ell \mathcal{C}_{\kappa_0}^{\ell'} \\ \frac{\mu_0}{\kappa_0} \mathbf{R}_\ell \mathcal{C}_{\kappa_0}^{\ell'} & \mathbf{R}_\ell \mathcal{M}_{\kappa_0}^{\ell'} \end{bmatrix} \begin{bmatrix} \boldsymbol{\psi}_{\ell'} \\ \boldsymbol{\varphi}_{\ell'} \end{bmatrix} = 2 \begin{bmatrix} \mathbf{g}_\ell \\ \mathbf{f}_\ell \end{bmatrix}. \end{aligned} \quad (16)$$

Remark 1. Let us compare the system matrix \mathbf{K}_{DM} of the direct method in (13) and the system matrix \mathbf{K}_{IM} of the indirect method in (16). Let ${}^\top \mathbf{K} := \overline{\mathbf{K}^* \mathbf{f}}$ denote the adjoint of an operator \mathbf{K} with respect to the bilinear rather than the

sesquilinear L^2 product and recall that ${}^\top \mathbf{M}_\kappa^\ell = \mathbf{R}_\ell \mathbf{M}_\kappa^\ell \mathbf{R}_\ell$ and ${}^\top \mathbf{C}_\kappa^\ell = \mathbf{R}_\ell \mathbf{C}_\kappa^\ell \mathbf{R}_\ell$. We set $\mathbf{R} = \text{diag} \left(\begin{bmatrix} \mathbf{R}_1 & 0 \\ 0 & \mathbf{R}_1 \end{bmatrix}, \dots, \begin{bmatrix} \mathbf{R}_N & 0 \\ 0 & \mathbf{R}_N \end{bmatrix} \right)$. Using this and the identity $\mathbf{R}^2 = -\mathbf{I}$ we find that

$${}^\top \mathbf{K}_{\text{IM}} = -\mathbf{R} \mathbf{K}_{\text{DM}} \mathbf{R}. \quad (17)$$

This relation is useful in the context of iterative regularisation methods for the inverse problem where both systems with the operator \mathbf{K}_{DM} and with the operator \mathbf{K}_{IM} have to be solved in each iteration step. If these operators are essentially represented by transposed matrices, then only one matrix has to be set up and only one LU decomposition has to be computed when the discrete linear systems are solved by Gaussian elimination.

It follows from the representation formula (5) and the ansatz (15) that the far-field pattern is computed via the integral representation formulas

$$\begin{aligned} \mathbf{E}^\infty &= \sum_{\ell=1}^N \mathbf{G}^\ell (\mathbf{u}_\ell^s + \mathbf{u}_\ell^{\text{inc}}) \quad \text{if one solves (13), or} \\ \mathbf{E}^\infty &= \sum_{\ell=1}^N \mathbf{G}^\ell \begin{bmatrix} \boldsymbol{\varphi}_\ell \\ \boldsymbol{\psi}_\ell \end{bmatrix} \quad \text{if one solves (16),} \end{aligned}$$

using the far-field operator $\mathbf{G}^\ell : (\mathbf{H}_{\text{div}}^{-1/2}(\Gamma_\ell))^2 \rightarrow \mathbf{L}_t^2(\mathbb{S}^2)$ defined for $\hat{\mathbf{x}} \in \mathbb{S}^2$ by

$$\begin{aligned} \mathbf{G}^\ell \begin{bmatrix} \boldsymbol{\varphi}_\ell \\ \boldsymbol{\psi}_\ell \end{bmatrix} (\hat{\mathbf{x}}) &= \frac{\mu_0}{4\pi} \int_{\Gamma_\ell} e^{-i\kappa_0 \hat{\mathbf{x}} \cdot \mathbf{y}} (\hat{\mathbf{x}} \times \boldsymbol{\psi}_\ell(\mathbf{y}) \times \hat{\mathbf{x}}) \, \text{ds}(\mathbf{y}) \\ &\quad + \frac{i\kappa_0}{4\pi} \int_{\Gamma_\ell} e^{-i\kappa_0 \hat{\mathbf{x}} \cdot \mathbf{y}} (\hat{\mathbf{x}} \times \boldsymbol{\varphi}_\ell(\mathbf{y})) \, \text{ds}(\mathbf{y}). \end{aligned}$$

Definition 2. Although in general $\mathbf{a} \times (\mathbf{b} \times \mathbf{c}) = (\mathbf{a} \cdot \mathbf{c})\mathbf{b} - (\mathbf{a} \cdot \mathbf{b})\mathbf{c}$ is different from $(\mathbf{a} \times \mathbf{b}) \times \mathbf{c}$ for $\mathbf{a}, \mathbf{b}, \mathbf{c} \in \mathbb{R}^3$, both expressions coincide for $\mathbf{a} = \mathbf{c}$. The unit vector $\mathbf{a} \times (\mathbf{b} \times \mathbf{a}) = (\mathbf{a} \times \mathbf{b}) \times \mathbf{a}$ is the orthogonal projection of \mathbf{b} onto the plane orthogonal to \mathbf{a} and is denoted by $\mathbf{a} \times \mathbf{b} \times \mathbf{a}$.

3 Spherical reformulation of the boundary integral equations

The first step in the derivation of our algorithm is to transport on the unit sphere \mathbb{S}^2 each of the integral equations on Γ_ℓ , for $\ell = 1, \dots, N$, derived in [Section 2](#).

We denote by θ, ϕ the spherical coordinates of any point $\hat{\mathbf{x}} \in \mathbb{S}^2$, that is,

$$\hat{\mathbf{x}} = \psi(\theta, \phi) = (\sin \theta \cos \phi, \sin \theta \sin \phi, \cos \theta), \quad (18)$$

for $(\theta, \phi) \in]0, \pi[\times]0, 2\pi[\cup \{(0, 0), (0, \pi)\}$. The tangent and the cotangent planes at any point $\hat{\mathbf{x}} = \psi(\theta, \phi) \in \mathbb{S}^2$ is generated by the unit vectors $\mathbf{e}_\theta = \frac{\partial \psi}{\partial \theta}(\theta, \phi)$ and $\mathbf{e}_\phi = \frac{1}{\sin \theta} \frac{\partial \psi}{\partial \phi}(\theta, \phi)$. The triplet $(\hat{\mathbf{x}}, \mathbf{e}_\theta, \mathbf{e}_\phi)$ forms an orthonormal system. The determinant of the Jacobian is $J_\psi(\theta, \phi) = \sin \theta$.

Let $\mathbf{q} : \mathbb{S}^2 \rightarrow \Gamma_\ell$ be a parametrisation of class \mathcal{C}^1 at least. We use the notation of [Appendix A](#). The total derivative $[D\mathbf{q}(\hat{\mathbf{x}})]$ maps the tangent plane $\mathbf{T}_{\hat{\mathbf{x}}}$ to \mathbb{S}^2 at the point $\hat{\mathbf{x}}$ onto the tangent plane $\mathbf{T}_{\mathbf{q}(\hat{\mathbf{x}})}$ to Γ_ℓ at the point $\mathbf{q}(\hat{\mathbf{x}})$. The latter is generated by the vectors

$$\begin{aligned} \mathbf{t}_1(\hat{\mathbf{x}}) &= \mathbf{e}_1(\mathbf{q}(\hat{\mathbf{x}})) = \frac{\partial \mathbf{q} \circ \psi}{\partial \theta} \circ \psi^{-1} = [D\mathbf{q}(\hat{\mathbf{x}})] \mathbf{e}_\theta, \\ \mathbf{t}_2(\hat{\mathbf{x}}) &= \frac{1}{J_\psi \circ \psi^{-1}(\hat{\mathbf{x}})} \mathbf{e}_2(\mathbf{q}(\hat{\mathbf{x}})) = \frac{1}{J_\psi \circ \psi^{-1}(\hat{\mathbf{x}})} \frac{\partial \mathbf{q} \circ \psi}{\partial \phi} \circ \psi^{-1} = [D\mathbf{q}(\hat{\mathbf{x}})] \mathbf{e}_\phi. \end{aligned}$$

The determinant $J_\mathbf{q}$ of the Jacobian of the change of variables $\mathbf{q} : \mathbb{S}^2 \rightarrow \Gamma_\ell$ and the normal vector $\mathbf{n}_\ell \circ \mathbf{q}$ is computed via

$$J_\mathbf{q} = \frac{J_{\mathbf{q} \circ \psi} \circ \psi^{-1}}{J_\psi \circ \psi^{-1}} = |\mathbf{t}_1 \times \mathbf{t}_2| \quad \text{and} \quad \mathbf{n}_\ell \circ \mathbf{q} = \frac{(\mathbf{e}_1 \circ \mathbf{q}) \times (\mathbf{e}_2 \circ \mathbf{q})}{J_{\mathbf{q} \circ \psi} \circ \psi^{-1}} = \frac{\mathbf{t}_1 \times \mathbf{t}_2}{J_\mathbf{q}}.$$

The parametrisation $\mathbf{q} : \mathbb{S}^2 \rightarrow \Gamma_\ell$ being a diffeomorphism, we set $[D\mathbf{q}(\hat{\mathbf{x}})]^{-1} = [D\mathbf{q}^{-1}] \circ \mathbf{q}(\hat{\mathbf{x}})$. The transposed matrix $[D\mathbf{q}(\hat{\mathbf{x}})^*]^{-1}$ maps the cotangent plane $\mathbf{T}_{\hat{\mathbf{x}}}^*$

to \mathbb{S}^2 at the point $\hat{\mathbf{x}}$ onto the cotangent plane $\mathbf{T}_{\mathbf{q}(\hat{\mathbf{x}})}^*$ to Γ_ℓ at the point $\mathbf{q}(\hat{\mathbf{x}})$. The latter is generated by the vectors

$$\begin{aligned} \mathbf{t}^1(\hat{\mathbf{x}}) &= \mathbf{e}^1(\mathbf{q}(\hat{\mathbf{x}})) = \frac{1}{J_{\mathbf{q} \circ \psi \circ \psi^{-1}}} \mathbf{e}_2(\mathbf{q}(\hat{\mathbf{x}})) \times \mathbf{n}_\ell(\mathbf{q}(\hat{\mathbf{x}})) \\ &= \frac{\mathbf{t}_2(\mathbf{q}(\hat{\mathbf{x}})) \times \mathbf{n}_\ell(\mathbf{q}(\hat{\mathbf{x}}))}{J_{\mathbf{q}}(\hat{\mathbf{x}})} = [\mathbf{D}\mathbf{q}(\hat{\mathbf{x}})^*]^{-1} \mathbf{e}_\theta, \\ \mathbf{t}^2(\hat{\mathbf{x}}) &= J_\psi \circ \psi^{-1}(\hat{\mathbf{x}}) \mathbf{e}^2(\mathbf{q}(\hat{\mathbf{x}})) = \frac{\mathbf{n}_\ell(\mathbf{q}(\hat{\mathbf{x}})) \times \mathbf{t}_1(\mathbf{q}(\hat{\mathbf{x}}))}{J_{\mathbf{q}}(\hat{\mathbf{x}})} = [\mathbf{D}\mathbf{q}(\hat{\mathbf{x}})^*]^{-1} \mathbf{e}_\phi. \end{aligned}$$

In view of the formulas (31)–(34), it is straightforward to deduce the following transformation formulas for the surface differential operators:

$$\begin{aligned} (\operatorname{grad}_{\Gamma_\ell} \mathbf{u}) \circ \mathbf{q} &= [\mathbf{D}\mathbf{q}^*]^{-1} \operatorname{grad}_{\mathbb{S}^2}(\mathbf{u} \circ \mathbf{q}), \\ (\operatorname{curl}_{\Gamma_\ell} \mathbf{u}) \circ \mathbf{q} &= \frac{1}{J_{\mathbf{q}}} [\mathbf{D}\mathbf{q}] \operatorname{curl}_{\mathbb{S}^2}(\mathbf{u} \circ \mathbf{q}), \\ (\operatorname{div}_{\Gamma_\ell} \mathbf{v}) \circ \mathbf{q} &= \frac{1}{J_{\mathbf{q}}} \operatorname{div}_{\mathbb{S}^2} (J_{\mathbf{q}} [\mathbf{D}\mathbf{q}]^{-1}(\mathbf{v} \circ \mathbf{q})), \\ (\operatorname{curl}_{\Gamma_\ell} \mathbf{w}) \circ \mathbf{q} &= \frac{1}{J_{\mathbf{q}}} \operatorname{curl}_{\mathbb{S}^2} ([\mathbf{D}\mathbf{q}^*](\mathbf{w} \circ \mathbf{q})). \end{aligned} \quad (19)$$

From this we now introduce a boundedly invertible operator from $\mathbf{H}_{\operatorname{div}}^{-1/2}(\Gamma_\ell)$ to $\mathbf{H}_{\operatorname{div}}^{-1/2}(\mathbb{S}^2)$. First recall that $\mathbf{H}_{\operatorname{div}}^{-1/2}(\Gamma_\ell)$ admits the Hodge decomposition [11]

$$\mathbf{H}_{\operatorname{div}}^{-1/2}(\Gamma_\ell) = \operatorname{grad}_{\Gamma_\ell} \mathbf{H}^{3/2}(\Gamma_\ell) \oplus \operatorname{curl}_{\Gamma_\ell} \mathbf{H}^{1/2}(\Gamma_\ell) \quad (20)$$

provided that the surface Γ_ℓ is smooth and simply connected. A first transformation, which intertwines with the Hodge decomposition, is the following:

$$\begin{aligned} \mathbf{H}_{\operatorname{div}}^{-1/2}(\Gamma_\ell) &\longrightarrow \mathbf{H}_{\operatorname{div}}^{-1/2}(\mathbb{S}^2) \\ \boldsymbol{\varphi} = \operatorname{grad}_{\Gamma_\ell} \mathbf{p}_1 + \operatorname{curl}_{\Gamma_\ell} \mathbf{p}_2 &\mapsto \boldsymbol{\varphi} = [\mathbf{D}\mathbf{q}^*](\operatorname{grad}_{\Gamma_\ell} \mathbf{p}_1) \circ \mathbf{q} \\ &\quad + J_{\mathbf{q}} [\mathbf{D}\mathbf{q}]^{-1}(\operatorname{curl}_{\Gamma_\ell} \mathbf{p}_2) \circ \mathbf{q} \\ &= \operatorname{grad}_{\mathbb{S}^2}(\mathbf{p}_1 \circ \mathbf{q}) + \operatorname{curl}_{\mathbb{S}^2}(\mathbf{p}_2 \circ \mathbf{q}). \end{aligned}$$

This transformation was first considered by Costabel and Le Louër [10] in the context of the shape differentiability analysis of the boundary integral operators M_κ and C_κ . However, for the numerical solution of boundary integral equations it is inconvenient as it requires explicit knowledge of the Hodge decomposition. Therefore, we use a second transformation, the so-called Piola transform of \mathbf{q} , introduced in the following Lemma 3.


Lemma 3. *The linear mapping*

$$\begin{aligned} \mathcal{P}_\mathbf{q} : \mathbf{H}_{\text{div}}^{-1/2}(\Gamma_\ell) &\longrightarrow \mathbf{H}_{\text{div}}^{-1/2}(\mathbb{S}^2) \\ \boldsymbol{\varphi} &\longmapsto \boldsymbol{\varphi} = J_\mathbf{q}[\mathbf{D}\mathbf{q}]^{-1}(\boldsymbol{\varphi} \circ \mathbf{q}). \end{aligned} \quad (21)$$

is well-defined and bounded and has a bounded inverse $\mathcal{P}_\mathbf{q}^{-1} : \mathbf{H}_{\text{div}}^{-1/2}(\mathbb{S}^2) \rightarrow \mathbf{H}_{\text{div}}^{-1/2}(\Gamma_\ell)$, $\mathcal{P}_\mathbf{q}^{-1}\boldsymbol{\varphi} = (\frac{1}{J_\mathbf{q}}[\mathbf{D}\mathbf{q}]\boldsymbol{\varphi}) \circ \mathbf{q}^{-1}$. Moreover $\mathcal{P}_\mathbf{q} \left(\text{Ker}[\text{div}_{\Gamma_\ell}(\mathbf{H}_t^{-1/2}(\Gamma_\ell))] \right) = \text{Ker}[\text{div}_{\mathbb{S}^2}(\mathbf{H}_t^{-1/2}(\mathbb{S}^2))]$.

Proof: To see that $\boldsymbol{\varphi}$ belongs to $\mathbf{H}_{\text{div}}^{-1/2}(\mathbb{S}^2)$, write $\boldsymbol{\varphi} = \text{grad}_{\Gamma_\ell} \mathbf{p}_1 + \text{curl}_{\Gamma_\ell} \mathbf{p}_2$ with $\mathbf{p}_1 \in H^{3/2}(\Gamma_\ell)$ and $\mathbf{p}_2 \in H^{1/2}(\Gamma_\ell)$ according to (20) and note that

$$\text{div}_{\mathbb{S}^2} J_\mathbf{q}[\mathbf{D}\mathbf{q}]^{-1}(\text{curl}_{\Gamma_\ell} \mathbf{p}_2) \circ \mathbf{q} = \text{div}_{\mathbb{S}^2} \text{curl}_{\mathbb{S}^2}(\mathbf{p}_2 \circ \mathbf{q}) = 0$$

using (37). As $J_\mathbf{q}[\mathbf{D}\mathbf{q}]^{-1}(\text{grad}_{\Gamma_\ell} \mathbf{p}_1) \circ \mathbf{q} \in \mathbf{H}^{1/2}(\mathbb{S}^2)$ it follows that $\text{div}_{\mathbb{S}^2} \boldsymbol{\varphi} \in \mathbf{H}^{-1/2}(\mathbb{S}^2)$, and $\boldsymbol{\varphi} \in \mathbf{H}_t^{-1/2}(\Gamma_\ell)$ implies $\boldsymbol{\varphi} \in \mathbf{H}_t^{-1/2}(\mathbb{S}^2)$. The boundedness of $\mathcal{P}_\mathbf{q}$ is straightforward. The proof for $\mathcal{P}_\mathbf{q}^{-1} = \mathcal{P}_{\mathbf{q}^{-1}}$ is analogous. 

We construct our spectral method by replacing the boundary integral operators M_κ^ℓ and C_κ^ℓ in (13) and (16) by the operators

$$\underline{M}_\kappa^\ell := \mathcal{P}_\mathbf{q} M_\kappa^\ell \mathcal{P}_\mathbf{q}^{-1} \quad \text{and} \quad \underline{C}_\kappa^\ell := \mathcal{P}_\mathbf{q} C_\kappa^\ell \mathcal{P}_\mathbf{q}^{-1}$$

which map $\mathbf{H}_{\text{div}}^{-1/2}(\mathbb{S}^2)$ boundedly into itself and are

$$\begin{aligned} \underline{\mathcal{M}}_{\kappa}^{\ell} \underline{\boldsymbol{\varphi}}_{\ell} &= J_{\mathbf{q}} [\mathbf{D}\mathbf{q}]^{-1} \int_{\mathbb{S}^2} (\mathbf{n}_{\ell} \circ \mathbf{q}) \times \mathbf{curl}\{2\Phi(\kappa, \mathbf{q}(\cdot) - \mathbf{q}(\hat{\mathbf{y}}))[\mathbf{D}\mathbf{q}(\hat{\mathbf{y}})]\underline{\boldsymbol{\varphi}}_{\ell}(\hat{\mathbf{y}})\} \mathbf{d}s(\hat{\mathbf{y}}), \\ \underline{\mathcal{C}}_{\kappa}^{\ell} \underline{\boldsymbol{\varphi}}_{\ell} &= \kappa J_{\mathbf{q}} [\mathbf{D}\mathbf{q}]^{-1} \int_{\mathbb{S}^2} (\mathbf{n}_{\ell} \circ \mathbf{q}) \times \{2\Phi(\kappa, \mathbf{q}(\cdot) - \mathbf{q}(\hat{\mathbf{y}}))[\mathbf{D}\mathbf{q}(\hat{\mathbf{y}})]\underline{\boldsymbol{\varphi}}_{\ell}(\hat{\mathbf{y}})\} \mathbf{d}s(\hat{\mathbf{y}}) \\ &+ \frac{1}{\kappa} J_{\mathbf{q}} [\mathbf{D}\mathbf{q}]^{-1} \int_{\mathbb{S}^2} (\mathbf{n}_{\ell} \circ \mathbf{q}) \times \text{grad div}\{2\Phi(\kappa, \mathbf{q}(\cdot) - \mathbf{q}(\hat{\mathbf{y}}))[\mathbf{D}\mathbf{q}(\hat{\mathbf{y}})]\underline{\boldsymbol{\varphi}}_{\ell}(\hat{\mathbf{y}})\} \mathbf{d}s(\hat{\mathbf{y}}). \end{aligned}$$

In our case we implement the compact operators $\underline{\mathcal{M}}_{\kappa_{\ell}}^{\ell}$, $\underline{\mathcal{M}}_{\kappa_0}^{\ell}$ and $\underline{\kappa_0 \mathcal{C}}_{\kappa_0}^{\ell} - \kappa_{\ell} \underline{\mathcal{C}}_{\kappa_{\ell}}^{\ell}$.

Let \mathbf{q}_{ℓ} and $\mathbf{q}_{\ell'}$ be the spherical parametrisations of two disjoint boundaries Γ_{ℓ} and $\Gamma_{\ell'}$. The operators $2\mathbf{R}_{\ell} \underline{\mathcal{M}}_{\kappa}^{\ell'}$ and $2\mathbf{R}_{\ell} \underline{\mathcal{C}}_{\kappa}^{\ell'}$ are replaced by the operators

$$\underline{\mathcal{M}}_{\kappa}^{\ell, \ell'} := 2\mathcal{P}_{\mathbf{q}_{\ell}} \mathbf{R}_{\ell} \underline{\mathcal{M}}_{\kappa}^{\ell'} \mathcal{P}_{\mathbf{q}_{\ell'}}^{-1} \quad \text{and} \quad \underline{\mathcal{C}}_{\kappa}^{\ell, \ell'} := 2\mathcal{P}_{\mathbf{q}_{\ell}} \mathbf{R}_{\ell} \underline{\mathcal{C}}_{\kappa}^{\ell'} \mathcal{P}_{\mathbf{q}_{\ell'}}^{-1}$$

defined by

$$\begin{aligned} \underline{\mathcal{M}}_{\kappa}^{\ell, \ell'} \underline{\boldsymbol{\varphi}}_{\ell'} &= J_{\mathbf{q}_{\ell}} [\mathbf{D}\mathbf{q}_{\ell}]^{-1} \int_{\mathbb{S}^2} (\mathbf{n}_{\ell} \circ \mathbf{q}_{\ell}) \\ &\quad \times \mathbf{curl}\{2\Phi(\kappa, \mathbf{q}_{\ell}(\cdot) - \mathbf{q}_{\ell'}(\hat{\mathbf{y}}))[\mathbf{D}\mathbf{q}_{\ell'}(\hat{\mathbf{y}})]\underline{\boldsymbol{\varphi}}_{\ell'}(\hat{\mathbf{y}})\} \mathbf{d}s(\hat{\mathbf{y}}), \\ \underline{\mathcal{C}}_{\kappa}^{\ell, \ell'} \underline{\boldsymbol{\varphi}}_{\ell'} &= \kappa J_{\mathbf{q}_{\ell}} [\mathbf{D}\mathbf{q}_{\ell}]^{-1} \int_{\mathbb{S}^2} (\mathbf{n}_{\ell} \circ \mathbf{q}_{\ell}) \\ &\quad \times \{2\Phi(\kappa, \mathbf{q}_{\ell}(\cdot) - \mathbf{q}_{\ell'}(\hat{\mathbf{y}}))[\mathbf{D}\mathbf{q}_{\ell'}(\hat{\mathbf{y}})]\underline{\boldsymbol{\varphi}}_{\ell'}(\hat{\mathbf{y}})\} \mathbf{d}s(\hat{\mathbf{y}}) \\ &+ \frac{1}{\kappa} J_{\mathbf{q}_{\ell}} [\mathbf{D}\mathbf{q}_{\ell}]^{-1} \int_{\mathbb{S}^2} (\mathbf{n}_{\ell} \circ \mathbf{q}_{\ell}) \\ &\quad \times \text{grad div}\{2\Phi(\kappa, \mathbf{q}_{\ell}(\cdot) - \mathbf{q}_{\ell'}(\hat{\mathbf{y}}))[\mathbf{D}\mathbf{q}_{\ell'}(\hat{\mathbf{y}})]\underline{\boldsymbol{\varphi}}_{\ell'}(\hat{\mathbf{y}})\} \mathbf{d}s(\hat{\mathbf{y}}). \end{aligned}$$

In our case we have to implement the smooth operators $\underline{\mathcal{M}}_{\kappa_0}^{\ell, \ell'}$, $\underline{\mathcal{C}}_{\kappa_0}^{\ell, \ell'}$ for all $\ell, \ell' = 1, \dots, \mathbf{N}$ with $\ell \neq \ell'$. The new unknowns are tangential vector densities in $\mathbf{H}_{\text{div}}^{-1/2}(\mathbb{S}^2)$ obtained by applying the operator (21) to the unknowns in (13) and (16).

The parametrised form of the far-field operator \mathbf{G}^ℓ is $\underline{\mathbf{G}}^\ell \begin{bmatrix} \underline{\boldsymbol{\varphi}}_\ell \\ \underline{\boldsymbol{\psi}}_\ell \end{bmatrix} = \underline{\mathbf{G}}_1^\ell \underline{\boldsymbol{\varphi}}_\ell + \underline{\mathbf{G}}_2^\ell \underline{\boldsymbol{\psi}}_\ell$ with

$$\begin{aligned} \left(\underline{\mathbf{G}}_1^\ell \underline{\boldsymbol{\varphi}}_\ell \right) (\hat{\mathbf{x}}) &= \frac{i\kappa_0}{4\pi} \int_{\mathbb{S}^2} e^{-i\kappa_0 \hat{\mathbf{x}} \cdot \mathbf{q}_\ell(\hat{\mathbf{y}})} \hat{\mathbf{x}} \times [\mathbf{D}\mathbf{q}_\ell(\hat{\mathbf{y}})] \underline{\boldsymbol{\varphi}}_\ell(\hat{\mathbf{y}}) \, d\mathbf{s}(\hat{\mathbf{y}}), \\ \left(\underline{\mathbf{G}}_2^\ell \underline{\boldsymbol{\psi}}_\ell \right) (\hat{\mathbf{x}}) &= \frac{\mu_0}{4\pi} \int_{\mathbb{S}^2} e^{-i\kappa_0 \hat{\mathbf{x}} \cdot \mathbf{q}_\ell(\hat{\mathbf{y}})} \hat{\mathbf{x}} \times [\mathbf{D}\mathbf{q}_\ell(\hat{\mathbf{y}})] \underline{\boldsymbol{\psi}}_\ell(\hat{\mathbf{y}}) \times \hat{\mathbf{x}} \, d\mathbf{s}(\hat{\mathbf{y}}). \end{aligned}$$

4 Fully discrete Galerkin method and examples

In this section we discuss the implementation of the spherical reformulation of the equations described above and present some results to show the accuracy of the method.

To solve the parametrised boundary integral equation systems we extend the spectral algorithm of Ganesh and Graham [12] to the vector case, which ensures spectrally accurate convergence of the discrete solution for second kind scalar integral equations. With an alternative method this was done by Ganesh and Hawkins [16] for the perfect conductor problem. For both of the boundary integral equation systems, it consists in the approximation of the $2N$ equations in the subspace $\mathbb{T}_n \subset \mathbf{H}_{\text{div}}^{-1/2}(\mathbb{S}^2)$ of finite dimension $2(n+1)^2 - 2$ spanned by the orthonormal tangential vector spherical harmonics $(\mathbf{y}_{l,j}^{(1)} = \frac{1}{\sqrt{l(l+1)}} \text{grad}_{\mathbb{S}^2} Y_{l,j})_{1 \leq l \leq n, |j| \leq l}$ and $(\mathbf{y}_{l,j}^{(2)} = \frac{1}{\sqrt{l(l+1)}} \text{curl}_{\mathbb{S}^2} Y_{l,j})_{1 \leq l \leq n, |j| \leq l}$ of degree at most n (Appendix B).

We denote by $(\cdot | \cdot)_n$ the discrete inner product [16, Eq. (3.9)] on \mathbb{T}_n and by \mathcal{O}_n the projection operators on \mathbb{T}_n [16, Eq. (3.11)] defined by Ganesh et al. The first step of the algorithm consists in interpolating the integrand of the boundary integral operators with a weakly singular kernel by (componentwise) series of scalar spherical harmonics of degree at most $n' = 2n + 1$ and $n \geq 5$. These values are the theoretical constraints required on n and n' for

convergence analysis [15, 16]. The resulting operators are labelled by the lower index \mathbf{n}' . In a second step we project all the operators on the solution space $\mathbb{T}_{\mathbf{n}}$ by applying $\mathcal{O}_{\mathbf{n}}$. Depending on the shape and size of the boundaries Γ_{ℓ} for $\ell = 1, \dots, \mathbf{N}$, we may need different order \mathbf{n}_{ℓ} of vector spherical harmonics to achieve similar accuracy. Any density in $\mathbb{T}_{\mathbf{n}_{\ell}}$ is uniquely determined by its $2[(\mathbf{n}_{\ell} + 1)^2 - 1]$ coefficients. Finally, the systems (13) and (16) are discretized into $\sum_{\ell=1}^{\mathbf{N}} 4((\mathbf{n}_{\ell} + 1)^2 - 1)$ equations for the $\sum_{\ell=1}^{\mathbf{N}} 4((\mathbf{n}_{\ell} + 1)^2 - 1)$ unknown coefficients by applying the scalar product $(\cdot | \mathbf{y}_{\mathbf{l},\mathbf{j}}^{(1)})_{\mathbf{n}_{\ell}}$ and $(\cdot | \mathbf{y}_{\mathbf{l},\mathbf{j}}^{(2)})_{\mathbf{n}_{\ell}}$, for $\mathbf{l} = 1, \dots, \mathbf{n}_{\ell}$ and $\mathbf{j} = -\mathbf{l}, \dots, \mathbf{l}$ to each equation.

The discrete approximation $\mathbf{M}_{\kappa}^{\ell, \ell'}$ of the operator $\underline{\mathbf{M}}_{\kappa, \mathbf{n}'_{\ell}}^{\ell}$ (when $\ell = \ell'$) or $\underline{\mathcal{M}}_{\kappa, \mathbf{n}'_{\ell'}}^{\ell, \ell'}$ is of the form

$$\mathbf{M}_{\kappa}^{\ell, \ell'} = \begin{bmatrix} \mathbf{M}_{1,1} & \mathbf{M}_{1,2} \\ \mathbf{M}_{2,1} & \mathbf{M}_{2,2} \end{bmatrix},$$

where $\mathbf{M}_{\mathbf{a},\mathbf{b}}$, for $\mathbf{a}, \mathbf{b} = 1, 2$ is a $((\mathbf{n}_{\ell} + 1)^2 - 1) \times ((\mathbf{n}_{\ell'} + 1)^2 - 1)$ matrix. The coefficients of $\mathbf{M}_{\mathbf{a},\mathbf{b}}$, for $1 \leq \mathbf{l} \leq \mathbf{n}_{\ell}$, $1 \leq \mathbf{l}' \leq \mathbf{n}_{\ell'}$, $|\mathbf{j}| \leq \mathbf{l}$ and $|\mathbf{j}'| \leq \mathbf{l}'$ are

$$\begin{aligned} \mathbf{M}_{\mathbf{a},\mathbf{b}}^{\mathbf{l}'\mathbf{j}'\mathbf{l}\mathbf{j}} &= (\mathcal{O}_{\mathbf{n}_{\ell}} \underline{\mathbf{M}}_{\kappa, \mathbf{n}'_{\ell}}^{\ell} \mathbf{y}_{\mathbf{l}',\mathbf{j}'}^{(\mathbf{a})}, \mathbf{y}_{\mathbf{l},\mathbf{j}}^{(\mathbf{b})})_{\mathbf{n}_{\ell}} \quad (\text{when } \ell = \ell') \text{ or} \\ \mathbf{M}_{\mathbf{a},\mathbf{b}}^{\mathbf{l}'\mathbf{j}'\mathbf{l}\mathbf{j}} &= (\mathcal{O}_{\mathbf{n}_{\ell}} \underline{\mathcal{M}}_{\kappa, \mathbf{n}'_{\ell'}}^{\ell, \ell'} \mathbf{y}_{\mathbf{l}',\mathbf{j}'}^{(\mathbf{a})}, \mathbf{y}_{\mathbf{l},\mathbf{j}}^{(\mathbf{b})})_{\mathbf{n}_{\ell}}. \end{aligned}$$

We use the same procedure to implement the discrete approximations $(\kappa_0 \mathbf{C}_{\kappa_0}^{\ell, \ell} - \kappa_{\ell} \mathbf{C}_{\kappa_{\ell}}^{\ell, \ell})$ and $\mathbf{C}_{\kappa_0}^{\ell, \ell'}$ of the operators $(\kappa_0 \mathbf{C}_{\kappa_0}^{\ell} - \kappa_{\ell} \mathbf{C}_{\kappa_{\ell}}^{\ell})$ and $\underline{\mathcal{C}}_{\kappa_0}^{\ell, \ell'}$, respectively.

The discrete approximations of the operators \mathbf{K}_{DM} and \mathbf{K}_{IM} in (13) and (16) are denoted by $\mathbf{K}_{\text{DM}} = \left(\mathbf{K}_{\text{DM}}^{\ell, \ell'} \right)_{1 \leq \ell, \ell' \leq \mathbf{N}}$ and $\mathbf{K}_{\text{IM}} = \left(\mathbf{K}_{\text{IM}}^{\ell, \ell'} \right)_{1 \leq \ell, \ell' \leq \mathbf{N}}$. The block matrices $\mathbf{K}_{\text{DM}}^{\ell, \ell'}$ and $\mathbf{K}_{\text{IM}}^{\ell, \ell'}$, where ℓ represents the line rank and ℓ' is the

column rank, are defined by

$$\mathbf{K}_{\text{DM}}^{\ell,\ell} = \begin{bmatrix} \left(1 + \frac{\mu_0 \kappa_\ell^2}{\mu_\ell \kappa_0^2}\right) \mathbf{I} & 0 \\ 0 & \left(1 + \frac{\mu_\ell}{\mu_0}\right) \mathbf{I} \end{bmatrix} - \begin{bmatrix} \mathbf{M}_{\kappa_0}^{\ell,\ell} - \frac{\mu_0 \kappa_\ell^2}{\mu_\ell \kappa_0^2} \mathbf{M}_{\kappa_\ell}^{\ell,\ell} & \frac{\mu_0}{\kappa_0^2} (\kappa_0 \mathbf{C}_{\kappa_0}^{\ell,\ell} - \kappa_\ell \mathbf{C}_{\kappa_\ell}^{\ell,\ell}) \\ \frac{1}{\mu_0} (\kappa_0 \mathbf{C}_{\kappa_0}^{\ell,\ell} - \kappa_\ell \mathbf{C}_{\kappa_\ell}^{\ell,\ell}) & \mathbf{M}_{\kappa_0}^{\ell,\ell} - \frac{\mu_\ell}{\mu_0} \mathbf{M}_{\kappa_\ell}^{\ell,\ell} \end{bmatrix},$$

$$\mathbf{K}_{\text{IM}}^{\ell,\ell} = \begin{bmatrix} \left(1 + \frac{\mu_0 \kappa_\ell^2}{\mu_\ell \kappa_0^2}\right) \mathbf{I} & 0 \\ 0 & \left(1 + \frac{\mu_\ell}{\mu_0}\right) \mathbf{I} \end{bmatrix} + \begin{bmatrix} \mathbf{M}_{\kappa_0}^{\ell,\ell} - \frac{\mu_0 \kappa_\ell^2}{\mu_\ell \kappa_0^2} \mathbf{M}_{\kappa_\ell}^{\ell,\ell} & \frac{1}{\mu_0} (\kappa_0 \mathbf{C}_{\kappa_0}^{\ell,\ell} - \kappa_\ell \mathbf{C}_{\kappa_\ell}^{\ell,\ell}) \\ \frac{\mu_0}{\kappa_0^2} (\kappa_0 \mathbf{C}_{\kappa_0}^{\ell,\ell} - \kappa_\ell \mathbf{C}_{\kappa_\ell}^{\ell,\ell}) & \mathbf{M}_{\kappa_0}^{\ell,\ell} - \frac{\mu_\ell}{\mu_0} \mathbf{M}_{\kappa_\ell}^{\ell,\ell} \end{bmatrix},$$

and for $\ell \neq \ell'$
$$\mathbf{K}_{\text{DM}}^{\ell,\ell'} = - \begin{bmatrix} \mathbf{M}_{\kappa_0}^{\ell,\ell'} & \frac{\mu_0}{\kappa_0} \mathbf{C}_{\kappa_0}^{\ell,\ell'} \\ \frac{\kappa_0}{\mu_0} \mathbf{C}_{\kappa_0}^{\ell,\ell'} & \mathbf{M}_{\kappa_0}^{\ell,\ell'} \end{bmatrix},$$

$$\mathbf{K}_{\text{IM}}^{\ell,\ell'} = \begin{bmatrix} \mathbf{M}_{\kappa_0}^{\ell,\ell'} & \frac{\kappa_0}{\mu_0} \mathbf{C}_{\kappa_0}^{\ell,\ell'} \\ \frac{\mu_0}{\kappa_0} \kappa_0 \mathbf{C}_{\kappa_0}^{\ell,\ell'} & \mathbf{M}_{\kappa_0}^{\ell,\ell'} \end{bmatrix}.$$

The discrete approximation of the right-hand side $2(\mathbf{g}_\ell, \mathbf{f}_\ell)$ on Γ_ℓ of one of the boundary integral equation system is the vector $2(\mathbf{g}_\ell, \mathbf{f}_\ell) = 2(\mathbf{g}_{\ell,1}, \mathbf{g}_{\ell,2}, \mathbf{f}_{\ell,1}, \mathbf{f}_{\ell,2})$ whose coefficients are

$$\mathbf{g}_k^{\text{lj}} = (\mathcal{O}_{n_\ell}(\mathcal{P}_{q_\ell} \mathbf{g}_\ell) | \mathbf{y}_{\text{lj}}^{(k)})_{n_\ell} \quad \text{and} \quad \mathbf{f}_k^{\text{lj}} = (\mathcal{O}_{n_\ell}(\mathcal{P}_{q_\ell} \mathbf{f}_\ell) | \mathbf{y}_{\text{lj}}^{(k)})_{n_\ell}$$

for $k = 1, 2$, $\text{l} = 1, \dots, n_\ell$ and $j = -\text{l}, \dots, \text{l}$.

The discrete approximation of $\underline{\mathbf{G}}^\ell$ evaluated at the N_{obs} observation points $\hat{\mathbf{x}}_{\text{obs}}^s \in \mathbb{S}^2$ is $\mathbf{G}^\ell = [\mathbf{G}_{1,1}^\ell \quad \mathbf{G}_{1,2}^\ell \quad \mathbf{G}_{2,1}^\ell \quad \mathbf{G}_{2,2}^\ell]$, where $\mathbf{G}_{\alpha,b}^\ell$, for $\alpha, b = 1, 2$ is a $3N_{\text{obs}} \times 2((n_\ell + 1)^2 - 1)$ matrix. The coefficients of $\mathbf{G}_{\alpha,b}^\ell$, for $\alpha, b = 1, 2$, $1 \leq \text{l} \leq n_\ell$, $|j| \leq \text{l}$ and $s = 1, \dots, N_{\text{obs}}$ are

$$\mathbf{G}_{1,b}^{s \text{ lj}} = \left(\underline{\mathbf{G}}_1^\ell \mathbf{y}_{\text{lj}}^{(b)} \right) (\hat{\mathbf{x}}_{\text{obs}}^s), \quad \mathbf{G}_{2,b}^{s \text{ lj}} = \left(\underline{\mathbf{G}}_2^\ell \mathbf{y}_{\text{lj}}^{(b)} \right) (\hat{\mathbf{x}}_{\text{obs}}^s).$$

Table 2, 3 and 4 and exhibits fast convergence for the far-field pattern \mathbf{E}^∞ for dielectric spheres and other boundaries with parametric representations given either in Table 1 or by Ganesh and Graham [12]. As a first test, using the indirect method, we compute the electric far-field denoted, $\mathbf{E}_{\text{ps}}^\infty$, created by an off-center point source located inside one of the dielectric particles: $\mathbf{E}^{\text{inc}}(\mathbf{x}) = \text{grad } \Phi(\kappa_0, \mathbf{x} - \mathbf{s}) \times \mathbf{p}$, $\mathbf{s} \in \Omega$, and $\mathbf{p} \in \mathbb{S}^2$. In this case the total exterior wave has to vanish so that the far-field pattern of the scattered wave \mathbf{E}^{s} is the opposite of the far-field pattern of the incident wave: $\mathbf{E}_{\text{exact}}^\infty(\hat{\mathbf{x}}) = -\frac{i\kappa_0}{4\pi} e^{-i\kappa_0 \hat{\mathbf{x}} \cdot \mathbf{s}} (\hat{\mathbf{x}} \times \mathbf{p})$. We choose $\mathbf{s} = (1, \frac{0.1}{2} - 1, \frac{0.1\sqrt{3}}{2} - 1)$ and $\mathbf{p} = (1, 0, 0)$. Table 2 lists the L^∞ error (by taking the maximum of errors obtained over 1300 observed directions, that is, we consider $N_{\text{obs}} = 2(\mathbf{n}_{\text{meas}} + 1)^2$ gauss quadrature points with $\mathbf{n}_{\text{meas}} = 25$).

As a second example, using the direct method, we compute the electric far-field denoted, $\mathbf{E}_{\text{pw}}^\infty$, created by the scattering of an incident plane wave. Table 2 shows the real part and the imaginary part of the polarisation component of the electric far-field evaluated at the incident direction: $[\mathbf{E}_{\text{pw}}^\infty(\mathbf{d})]_{\mathbf{n}} \cdot \mathbf{p}$. We choose $\mathbf{d} = (0, -1, 0)$ and $\mathbf{p} = (1, 0, 0)$. In the case of the sphere, the analytical representation of the far-field pattern is given by a Mie series [39], then Table 3 and Table 4 indicates the L^∞ error.

The experiments were realised with MATLAB programming language using parallel for-loops for the matrix setup. In the resonance region (with a wavelength close to the size of the obstacles) and with a small number of obstacles, the simulation of an accurate approximate solution takes from a few seconds to a few minutes of CPU time using a 2.67 GHz Intel Xeon processor with 20 workers. This is illustrated in Table 2 where the scattering by four dielectric particles is considered. The exterior parameters are $\kappa_0 = \pi$ and $\mu_0 = 1$. Inside the peanut $\mu_1 = 1$ and $\kappa_1 = 1.2\kappa_0$, whereas inside the bean $\mu_2 = 0.9$ and $\kappa_2 = 2\kappa_0$, inside the rectangle $\mu_3 = 1.1$, $\kappa_3 = 1.5\kappa_0$, and inside the tetrahedron $\mu_4 = 1.5$, $\kappa_4 = 0.7\kappa_0$. All these obstacles have a diameter close to half of the wavelength $\mathfrak{l} = \frac{2\pi}{\kappa_0} = 2$. The separation distance between the particles varies between $0.5\mathfrak{l}$ and $1.5\mathfrak{l}$. The results show that by setting $\mathbf{n} \approx 10$ for the four obstacles one generates synthetic data, that are used in

Table 1: Parametric representation of the dielectric interfaces for various surfaces [12, 44]

peanut $\mathbf{q}_1 \circ \psi(\theta, \phi) = (-1, 1, 0) + r(\theta)(\sin \theta \cos \phi, 2 \sin \theta \sin \phi, \cos \theta),$

$$r(\theta) = 0.5(1 + \sqrt{1.25})^{-1/2} (\cos(2\theta) + \sqrt{1 + \cos^2(2\theta)})^{\frac{1}{2}};$$

bean $\mathbf{q}_2 \circ \psi(\theta, \phi) =$

$$(0, 0, 2) + 0.6(A(\theta) \sin \theta \cos \phi, B(\theta) \sin \theta \sin \phi - .3C(\theta), \cos \theta),$$

$$A(\theta) = \sqrt{.64(1 - .1C(\theta))}, B(\theta) = \sqrt{.64(1 - .4C(\theta))},$$

$$C(\theta) = \cos(\pi \cos \theta);$$

rounded rectangle $\mathbf{q}_3 \circ \psi(\theta, \phi) =$

$$(1, -1, -1) + r(\theta, \phi)(0.4 \sin \theta \cos \phi, 0.6 \sin \theta \sin \phi, 0.4 \cos \theta)$$

$$r(\theta, \phi) = (|\sin \theta \cos \phi|^p + |\sin \theta \sin \phi|^p + |\cos \theta|^p)^{-\frac{1}{p}}, p = 8;$$

rounded tetrahedron $\mathbf{q}_4 \circ \psi(\theta, \phi) = (-1, -2, -1) + 0.5r(\theta, \phi)\psi(\theta, \phi),$

$$r(\theta, \phi) = (H(\gamma, \gamma, \gamma) + (\frac{1}{p})^{p-2}H(-\gamma, -\gamma, -\gamma))^{-\frac{1}{p}}, H(\gamma, \gamma, \gamma) =$$

$$h(\gamma, \gamma, \gamma)^p + h(-\gamma, -\gamma, \gamma)^p + h(-\gamma, \gamma, -\gamma)^p + h(\gamma, -\gamma, -\gamma)^p,$$

$$h(a, b, c) = |\min(0, a \sin \theta \cos \phi + b \sin \theta \sin \phi + c \cos \theta)|, \gamma = \frac{1}{\sqrt{3}},$$

$$p = 6;$$

stellated dodecahedron $\mathbf{q}_5 \circ \psi(\theta, \phi) = (0, 0, 0) + 0.2 r(\theta, \phi)\psi(\theta, \phi),$

where $r(\theta, \phi) > 0$ solves

$$p^{-|r(\theta, \phi)f(\delta, \xi, 0)|^p} + p^{-|r(\theta, \phi)f(\delta, -\xi, 0)|^p} + p^{-|r(\theta, \phi)f(0, \delta, \xi)|^p} +$$

$$p^{-|r(\theta, \phi)f(0, \delta, -\xi)|^p} + p^{-|r(\theta, \phi)f(\xi, 0, \delta)|^p} + p^{-|r(\theta, \phi)f(-\xi, 0, \delta)|^p} = 2.5, \text{ with}$$

$$f(a, b, c) = a \sin \theta \cos \phi + b \sin \theta \sin \phi + c \cos \theta, \delta = \sqrt{\frac{5-\sqrt{5}}{10}},$$

$$\xi = \sqrt{\frac{5+\sqrt{5}}{10}}, p = 3.4;$$

Table 2: Convergence of the forward solver for the dielectric scattering problem by the first four obstacles described in Table 1. The second column displays the error of the far-field pattern for an interior point source and the next two columns display point values of the far-field pattern for a plane incident wave.

n	$\ [\mathbf{E}_{\text{ps}}^\infty]_n - \mathbf{E}_{\text{exact}}^\infty\ _\infty$	$\Re[\mathbf{E}_{\text{pw}}^\infty(\mathbf{d})]_n \cdot \mathbf{p}$	$\Im[\mathbf{E}_{\text{pw}}^\infty(\mathbf{d})]_n \cdot \mathbf{p}$	CPU
10	2.02E-03	1.050 718	1.165 611	4 min
20	2.74E-05	1.054 709	1.170 534	25 min
30	5.44E-07	1.054 838	1.170 756	96 min
40	8.38E-09	1.054 839	1.170 756	276 min

Section 7, with a precision close to 10^{-3} .

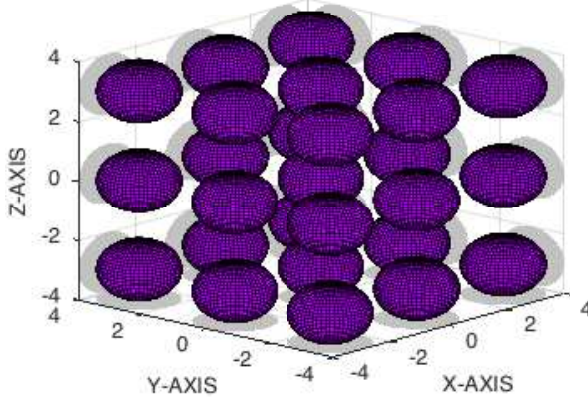
5 Operator formulations and IRGN method

To make the operator formulation (2) in the introduction precise, we first introduce a set of admissible parametrisations \mathcal{V} which forms an open subset of a Hilbert space \mathcal{X} . As in the introduction, let $F_j : \mathcal{V}^N \rightarrow \mathbf{L}_t^2(\mathbb{S}^2)$, $j = 1, \dots, m$ denote the operator which maps a sequence of parametrisations $\mathbf{q} := (\mathbf{q}_\ell)_{1 \leq \ell \leq N} \in \mathcal{V}^N$ of the union of boundaries $(\Gamma_\ell)_{1 \leq \ell \leq N}$ to the far-field pattern \mathbf{E}_j^∞ corresponding to the incident field $\mathbf{E}_j^{\text{inc}}$. These operators may be combined into one operator $F : \mathcal{V}^N \rightarrow \mathbf{L}_t^2(\mathbb{S}^2)^m$, $F(\mathbf{q}) := (F_1(\mathbf{q}), \dots, F_m(\mathbf{q}))$. We also combine the measured far-field patterns into a vector $\mathbf{E}_\delta^\infty := (\mathbf{E}_{1,\delta}^\infty, \dots, \mathbf{E}_{m,\delta}^\infty) \in \mathbf{L}_t^2(\mathbb{S}^2)^m$ such that the inverse problem is written as

$$F(\mathbf{q}) = \mathbf{E}_\delta^\infty. \quad (22)$$

Table 3: Convergence of the forward solver for the scattering problem by 27 dielectric spheres. Their diameters are given between brackets. The separation distance between the obstacles is about $0.5\mathbf{l}$.

$27 \times \text{sphere}(1\mathbf{l}), \kappa_\ell = 2\kappa_0 = 2\pi, \mu_0 = \mu_\ell = 1$		
n	$\ [\mathbf{E}_{\text{pw}}^\infty]_n - \mathbf{E}_{\text{exact}}^\infty\ _\infty$	CPU time
5	8.96E-03	21 min
10	2.12E-07	94 min
15	1.60E-11	310 min



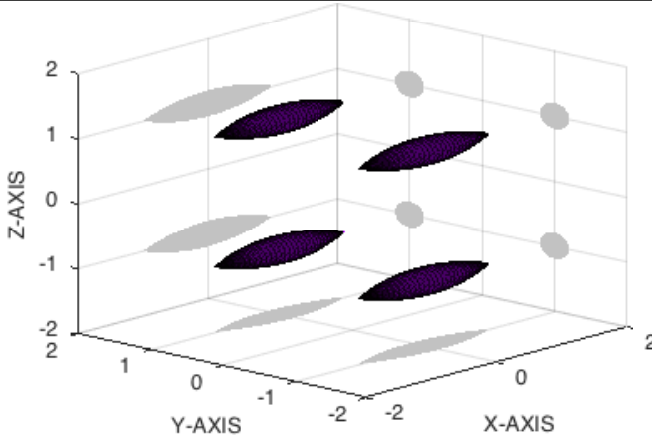
To compute an approximate solution to (22) we use the Iteratively Regularized Gauss–Newton method for Hilbert spaces [27, 28]. To apply this method we show in Section 6 that the operator F is Fréchet differentiable and derive formulas to evaluate the Fréchet derivative $F'[\mathbf{q}]$ and its adjoint $F'[\mathbf{q}]^*$. Then the iterates of the Iteratively Regularized Gauss–Newton method are computed by

$$\mathbf{q}_\delta^{k+1} := \arg \min_{\mathbf{q} \in \mathcal{X}^N} \left[\|F(\mathbf{q}_\delta^k) + F'[\mathbf{q}_\delta^k](\mathbf{q} - \mathbf{q}_\delta^k) - \mathbf{E}_\delta^\infty\|_{\mathbb{L}_t^2(\mathbb{S}^2)^m}^2 + \alpha_\kappa \|\mathbf{q} - \mathbf{q}^0\|^2 \right]. \quad (23)$$

Here $\mathbf{q}^0 = \mathbf{q}_\delta^0$ is some initial guess (in our numerical experiments we always chose the unit sphere), and the regularisation parameters are chosen of the

Table 4: Convergence of the forward solver for the scattering problem by four ogives. Their diameters are given between brackets. The separation distance between the obstacles is about $0.5\mathbf{l}$.

$4 \times \mathbf{ogive}(2\mathbf{l}), \kappa_\ell = 4\kappa_0 = 2\pi, \mu_0 = \mu_\ell = 1$		
n	$\ [\mathbf{E}_{\text{ps}}^\infty]_n - \mathbf{E}_{\text{exact}}^\infty\ _\infty$	CPU time
25	2.90E-03	31 min
35	1.55E-04	120 min
45	8.38E-06	267 min



form $\alpha_k = \alpha_0 \left(\frac{2}{3}\right)^k$ which provides logarithmic convergence rates of the Iteratively Regularized Gauss–Newton method [28, Theorem 4.9] when the stopping rule is given by the Morozov’s discrepancy principle (30). Since the objective functional in (23) is quadratic and strictly convex, the first order optimality conditions are necessary and sufficient, and the updates $(\partial \mathbf{q})^k := \mathbf{q}_\delta^{k+1} - \mathbf{q}_\delta^k$ are the unique solutions to the linear equations

$$\alpha_k \mathbf{I} + \mathbf{F}'[\mathbf{q}_\delta^k]^* \mathbf{F}'[\mathbf{q}_\delta^k] (\partial \mathbf{q})_\delta^k = \mathbf{F}'[\mathbf{q}_\delta^k]^* (\mathbf{E}_\delta^\infty - \mathbf{F}(\mathbf{q}_\delta^k)) + \alpha_k (\mathbf{q}_\delta^0 - \mathbf{q}_\delta^k). \quad (24)$$

It remains to describe the choice of the set of admissible parametrisations \mathcal{V}

and the underlying Hilbert space \mathcal{X} . A rather general way to parametrise a boundary Γ_ℓ is to choose some reference domain Ω_{ref} with boundary Γ_{ref} and consider mappings $\mathbf{q}_\ell : \Gamma_{\text{ref}} \rightarrow \Gamma_\ell$ belonging to

$$\mathcal{Q} := \left\{ \mathbf{q}_\ell \in \mathbf{H}^s(\Gamma_{\text{ref}}, \mathbb{R}^3) : \mathbf{q}_\ell \text{ injective, } \det(\mathbf{D}\mathbf{q}_\ell(\hat{\mathbf{x}})) \neq 0 \text{ for all } \hat{\mathbf{x}} \in \Gamma_{\text{ref}} \right\}. \quad (25)$$

This is convenient for describing Fréchet derivatives of \mathbf{F} in [Section 6](#). For $s > 2$ the set \mathcal{Q} is open in $\mathcal{X} := \mathbf{H}^s(\Gamma_{\text{ref}}, \mathbb{R}^3)$ and $\mathcal{X} \subset \mathcal{C}^1(\Gamma_{\text{ref}}, \mathbb{R}^3)$. If Γ_ℓ and Γ_{ref} are sufficiently smooth, then Γ_ℓ has a parametrisation in \mathcal{Q} if and only if Γ_ℓ and Γ_{ref} have the same genus.

A disadvantage of the choice (25) is that a given interface Γ_ℓ has many parametrisations in \mathcal{Q} . In the important special case that Γ_ℓ is star-shaped, we choose $\Gamma_{\text{ref}} = \mathbb{S}^2$ and consider special parametrisations of the form

$$\mathbf{q}_\ell = \mathbf{c}_\ell + \mathcal{R}\mathbf{r}_\ell \quad \text{with} \quad (\mathcal{R}\mathbf{r})(\hat{\mathbf{x}}) := r(\hat{\mathbf{x}})\hat{\mathbf{x}}, \quad \hat{\mathbf{x}} \in \mathbb{S}^2$$

with an unknown function $r_\ell : \mathbb{S}^2 \rightarrow (0, \infty)$ and a known location $\mathbf{c}_\ell \in \mathbb{R}^3$. Then the function r_ℓ is uniquely determined by Γ_ℓ . In this case we choose the underlying Hilbert space $\mathcal{X}_{\text{star}} := \mathbf{H}^s(\mathbb{S}^2, \mathbb{R})$ with $s > 2$ and the set of admissible parametrisations by

$$\mathcal{Q}_{\text{star}} := \{ \mathbf{r} \in \mathcal{X}_{\text{star}} : \mathbf{r} > 0 \}.$$

As $\mathcal{R}(\mathcal{Q}_{\text{star}}) \subset \mathcal{Q}$, we define $\mathbf{F}_{\text{star}} : \mathcal{Q}_{\text{star}}^{\mathbf{N}} \rightarrow \mathbf{L}_t^2(\mathbb{S}^2)^m$ by

$$\mathbf{F}_{\text{star}} := \mathbf{F} \circ (\mathcal{R}\mathbf{q}_\ell)_{1 \leq \ell \leq \mathbf{N}}.$$

Then \mathbf{F}_{star} is injective if the union of star-shaped interface $(\Gamma_\ell)_{1 \leq \ell \leq \mathbf{N}}$ is uniquely determined by the far-field data $\mathbf{E}_1^\infty, \dots, \mathbf{E}_m^\infty$.

6 The Fréchet derivative and its adjoint

In this section we assume that the set \mathcal{Q} of admissible parametrisations chosen by (25) with some reference boundary Γ_{ref} . For $\mathbf{q} := (\mathbf{q}_\ell)_{1 \leq \ell \leq \mathbf{N}} \in \mathcal{Q}^{\mathbf{N}}$ we define

$\Gamma_{\mathbf{q}_\ell} = \mathbf{q}_\ell(\Gamma_{\text{ref}})$, then $\Gamma_{\mathbf{q}} := \cup_{\ell=1}^N \Gamma_{\mathbf{q}_\ell}$, and we denote by $\mathbf{n}_{\mathbf{q}_\ell}$ the exterior unit normal vector to $\Gamma_{\mathbf{q}_\ell}$. More generally we label all quantities and operators related to the dielectric scattering problem for the boundary $\Gamma_{\mathbf{q}_\ell}$ by the index \mathbf{q}_ℓ . We restrict our discussion to the case $\mathbf{m} = 1$ since the general case is reduced to this special case by the formulas $F'[\mathbf{q}]\xi = (F'_1[\mathbf{q}]\xi, \dots, F'_m[\mathbf{q}]\xi)$ and $F'[\mathbf{q}]^*\mathbf{h} = \sum_{j=1}^m F'_j[\mathbf{q}]^*\mathbf{h}$.

The following theorem was established by Costabel and Le Louër [10] for the scattering problem by a single dielectric obstacle. An alternative proof was proposed by Hettlich [26].

Theorem 4 (characterisation of $F'[\mathbf{q}]$). *The mapping $F: \mathcal{Q}^N \rightarrow \mathbf{L}_t^2(\mathbf{S}^2)$ with $s > 2$ is Fréchet differentiable at all $\mathbf{q} \in \mathcal{Q}^N$ for which $\Gamma_{\mathbf{q}}$ is of class \mathcal{C}^2 , and the first derivative at \mathbf{q} in the direction $\xi := (\xi_\ell)_{1 \leq \ell \leq N} \in \mathcal{X}^N$ is*

$$F'[\mathbf{q}]\xi = \mathbf{E}_{\mathbf{q},\xi}^\infty,$$

where $\mathbf{E}_{\mathbf{q},\xi}^\infty$ is the far-field pattern of the solution $((\mathbf{E}_{\mathbf{q},\xi}^\ell)_{1 \leq \ell \leq N}, \mathbf{E}_{\mathbf{q},\xi}^s)$ to the Maxwell equations (1a) in $\mathbb{R}^3 \setminus \Gamma_{\mathbf{q}}$ that satisfies the Silver–Müller radiation condition and the transmissions condition on $\Gamma_{\mathbf{q}_\ell}$

$$\begin{aligned} \mathbf{n}_{\mathbf{q}_\ell} \times \mathbf{E}_{\mathbf{q},\xi}^s - \mathbf{n}_{\mathbf{q}_\ell} \times \mathbf{E}_{\mathbf{q},\xi}^\ell &= \mathbf{f}'_{\mathbf{q}_\ell, \xi_\ell}, \\ \frac{1}{\mu_0} \mathbf{n}_{\mathbf{q}_\ell} \times \mathbf{curl} \mathbf{E}_{\mathbf{q},\xi}^s - \frac{1}{\mu_\ell} \mathbf{n}_{\mathbf{q}_\ell} \times \mathbf{curl} \mathbf{E}_{\mathbf{q},\xi}^\ell &= \mathbf{g}'_{\mathbf{q}_\ell, \xi_\ell}, \end{aligned}$$

with

$$\begin{aligned}
\mathbf{f}'_{\mathbf{q}_\ell, \xi_\ell} &= -(\xi_\ell \circ \mathbf{q}_\ell^{-1} \cdot \mathbf{n}_{\mathbf{q}_\ell}) \left\{ \mathbf{n}_{\mathbf{q}_\ell} \times \mathbf{curl}(\mathbf{E}_{\mathbf{q}}^s + \mathbf{E}^{inc})|_{\Gamma_{\mathbf{q}_\ell}} \times \mathbf{n}_{\mathbf{q}_\ell} \right. \\
&\quad \left. - \mathbf{n}_{\mathbf{q}_\ell} \times \mathbf{curl} \mathbf{E}_{\mathbf{q}|_{\Gamma_{\mathbf{q}_\ell}}^\ell} \times \mathbf{n}_{\mathbf{q}_\ell} \right\} \\
&\quad + \mathbf{curl}_{\Gamma_{\mathbf{q}_\ell}} \left((\xi_\ell \circ \mathbf{q}_\ell^{-1} \cdot \mathbf{n}_{\mathbf{q}_\ell}) (\mathbf{n}_{\mathbf{q}_\ell} \cdot (\mathbf{E}_{\mathbf{q}}^s + \mathbf{E}^{inc})|_{\Gamma_{\mathbf{q}_\ell}} - \mathbf{n}_{\mathbf{q}_\ell} \cdot \mathbf{E}_{\mathbf{q}|_{\Gamma_{\mathbf{q}_\ell}}^\ell}) \right), \\
\mathbf{g}'_{\mathbf{q}_\ell, \xi_\ell} &= -(\xi_\ell \circ \mathbf{q}_\ell^{-1} \cdot \mathbf{n}_{\mathbf{q}_\ell}) \left\{ \frac{\kappa_0^2}{\mu_0} \mathbf{n}_{\mathbf{q}_\ell} \times (\mathbf{E}_{\mathbf{q}}^s + \mathbf{E}^{inc})|_{\Gamma_{\mathbf{q}_\ell}} \times \mathbf{n}_{\mathbf{q}_\ell} \right. \\
&\quad \left. - \frac{\kappa_\ell^2}{\mu_\ell} (\mathbf{n}_{\mathbf{q}_\ell} \times \mathbf{E}_{\mathbf{q}|_{\Gamma_{\mathbf{q}_\ell}}^\ell} \times \mathbf{n}_{\mathbf{q}_\ell}) \right\} \\
&\quad + \mathbf{curl}_{\Gamma_{\mathbf{q}_\ell}} \left((\xi_\ell \circ \mathbf{q}_\ell^{-1} \cdot \mathbf{n}_{\mathbf{q}_\ell}) \left\{ \frac{1}{\mu_0} \mathbf{n}_{\mathbf{q}_\ell} \cdot \mathbf{curl}(\mathbf{E}_{\mathbf{q}}^s + \mathbf{E}^{inc})|_{\Gamma_{\mathbf{q}_\ell}} \right. \right. \\
&\quad \left. \left. - \frac{1}{\mu_\ell} \mathbf{n}_{\mathbf{q}_\ell} \cdot \mathbf{curl} \mathbf{E}_{\mathbf{q}|_{\Gamma_{\mathbf{q}_\ell}}^\ell} \right\} \right)
\end{aligned}$$

where $((\mathbf{E}_{\mathbf{q}}^\ell)_{1 \leq \ell < n}, \mathbf{E}_{\mathbf{q}}^s)$ is the solution to the dielectric scattering problem (1a)–(1e) with the boundary $\Gamma_{\mathbf{q}}$ and we use [Definition 2](#).

Remark 5 (alternative form of boundary values). By straightforward calculations and the use of the transmission conditions, one expresses the boundary values of the Fréchet derivative in terms of the solution to the system of integral equations (13) of the direct approach, that is

$$\begin{bmatrix} \mathbf{u}_{\mathbf{q}, \ell}^{(1)} \\ \mathbf{u}_{\mathbf{q}, \ell}^{(2)} \end{bmatrix} = \mathbf{u}_{\mathbf{q}, \ell}^s + \mathbf{u}_\ell^{inc} = \begin{bmatrix} \mathbf{n}_{\mathbf{q}_\ell} \times (\mathbf{E}_{\mathbf{q}}^s + \mathbf{E}^{inc})|_{\Gamma_{\mathbf{q}_\ell}} \\ \frac{1}{\mu_0} \mathbf{n}_{\mathbf{q}_\ell} \times \mathbf{curl}(\mathbf{E}_{\mathbf{q}}^s + \mathbf{E}^{inc})|_{\Gamma_{\mathbf{q}_\ell}} \end{bmatrix}. \quad (26)$$

First $(\mathbf{E}_{\mathbf{q}}^s + \mathbf{E}^{inc}) = \frac{1}{\kappa_0^2} \mathbf{curl} \mathbf{curl}(\mathbf{E}_{\mathbf{q}}^s + \mathbf{E}^{inc})$ and $\mathbf{E}_{\mathbf{q}|_{\Omega_{\mathbf{q}_\ell}}^\ell} = \frac{1}{\kappa_\ell^2} \mathbf{curl} \mathbf{curl} \mathbf{E}_{\mathbf{q}|_{\Omega_{\mathbf{q}_\ell}}^\ell}$. Moreover, using the identity (see (35), (36))

$$\mathbf{n}_{\mathbf{q}} \cdot \mathbf{curl} \mathbf{E} = \mathbf{curl}_{\Gamma_{\mathbf{q}}}(\mathbf{n}_{\mathbf{q}} \times \mathbf{E} \times \mathbf{n}_{\mathbf{q}}) = -\operatorname{div}_{\Gamma_{\mathbf{q}}}(\mathbf{n}_{\mathbf{q}} \times \mathbf{E}) \quad \text{on } \Gamma_{\mathbf{q}}, \quad (27)$$

which holds for any smooth vector function \mathbf{E} defined on a neighborhood

of $\Gamma_{\mathbf{q}}$, we obtain

$$\begin{aligned} \mathbf{f}'_{\mathbf{q}_\ell, \xi_\ell} &= -(\boldsymbol{\xi}_\ell \circ \mathbf{q}_\ell^{-1} \cdot \mathbf{n}_{\mathbf{q}_\ell}) (\mu_0 - \mu_\ell) \mathbf{u}_{\mathbf{q}, \ell}^{(2)} \times \mathbf{n}_{\mathbf{q}_\ell} \\ &\quad - \left(\frac{\mu_0}{\kappa_0^2} - \frac{\mu_\ell}{\kappa_\ell^2} \right) \mathbf{curl}_{\Gamma_{\mathbf{q}_\ell}} \left(\boldsymbol{\xi}_{\mathbf{n}_{\mathbf{q}_\ell}} \operatorname{div}_{\Gamma_{\mathbf{q}_\ell}} \mathbf{u}_{\mathbf{q}, \ell}^{(2)} \right) \\ \mathbf{g}'_{\mathbf{q}_\ell, \xi_\ell} &= -(\boldsymbol{\xi}_\ell \circ \mathbf{q}_\ell^{-1} \cdot \mathbf{n}_{\mathbf{q}_\ell}) \left(\frac{\kappa_0^2}{\mu_0} - \frac{\kappa_\ell^2}{\mu_\ell} \right) \mathbf{u}_{\mathbf{q}, \ell}^{(1)} \times \mathbf{n}_{\mathbf{q}_\ell} \\ &\quad - \left(\frac{1}{\mu_0} - \frac{1}{\mu_\ell} \right) \mathbf{curl}_{\Gamma_{\mathbf{q}_\ell}} \left(\boldsymbol{\xi}_{\mathbf{n}_{\mathbf{q}_\ell}} \operatorname{div}_{\Gamma_{\mathbf{q}_\ell}} \mathbf{u}_{\mathbf{q}, \ell}^{(1)} \right). \end{aligned} \quad (28)$$

An interesting feature of these formulas is that they depend on the relative dielectric constants. For any obstacle Ω_ℓ whose parameters μ_ℓ and κ_ℓ are very close to μ_0 and κ_0 , then the Fréchet derivative of the far-field varies little under any deformation of Γ_ℓ (at least for the first iterations of the algorithm). We guess that in this case the shape reconstruction of this obstacle is rather slow with Iteratively Regularized Gauss–Newton method (illustrated in [Figure 1\(d\)](#)).

To define the adjoint of $F'[\mathbf{q}] : (\mathcal{X} = \mathbf{H}^s(\Gamma_{\text{ref}}; \mathbb{R}^3))^{\mathbb{N}} \rightarrow \mathbf{L}_t^2(\mathbb{S}^2)$, we interpret the naturally complex Hilbert space $\mathbf{L}_t^2(\mathbb{S}^2)$ as a real Hilbert space with the real-valued inner product $\Re \langle \cdot, \cdot \rangle_{\mathbf{L}_t^2(\mathbb{S}^2)}$. For bounded linear operator between complex Hilbert spaces such a reinterpretation of the spaces as real Hilbert spaces does not change the adjoint.

Proposition 6 (characterisation of the adjoint $F'[\mathbf{q}]^*$). *Let*

$$\mathbf{E}_{\mathbf{h}}^{\text{inc}}(\mathbf{y}) := \frac{\mu_0}{4\pi} \int_{\mathbb{S}^2} e^{-i\kappa_0 \hat{\mathbf{x}} \cdot \mathbf{y}} \mathbf{h}(\hat{\mathbf{x}}) \, ds(\hat{\mathbf{x}}), \quad \mathbf{y} \in \mathbb{R}^3, \quad (29)$$

denote the vector Herglotz function with kernel $\mathbf{h} \in \mathbf{L}_t^2(\mathbb{S}^2)$ and $\mathbf{E}_{\mathbf{q}, \bar{\mathbf{h}}}$ the total wave solution to the scattering problem for the dielectric interface $\Gamma_{\mathbf{q}}$ and the incident wave $\mathbf{E}_{\mathbf{h}}^{\text{inc}}$. Moreover, let $\mathfrak{j}_{\mathcal{X} \hookrightarrow \mathbf{L}^2}$ denote the embedding operator from

$\mathcal{X} = \mathbf{H}^s(\Gamma_{\text{ref}}, \mathbb{R}^3)$ to $\mathbf{L}^2(\Gamma_{\text{ref}}, \mathbb{R}^3)$. Then

$$\begin{aligned} F'[\mathbf{q}]^* \mathbf{h} &= (\boldsymbol{\xi}_{\ell, \mathbf{h}}^*)_{1 \leq \ell \leq N} \quad \text{where for } \ell = 1, \dots, N \\ \boldsymbol{\xi}_{\ell, \mathbf{h}}^* &= \mathbf{j}_{\mathcal{X} \hookrightarrow \mathbf{L}^2}^* \left[\mathbf{J}_{\mathbf{q}_\ell} \left(\mathbf{n}_{\mathbf{q}_\ell} \mathfrak{R} \left\{ -(\mu_0 - \mu_\ell) \left(\frac{1}{\mu_0} \mathbf{n}_{\mathbf{q}} \times \mathbf{curl} \overline{\mathbf{E}}_{\mathbf{q}, \bar{\mathbf{h}}} \right) \Big|_{\Gamma_{\mathbf{q}_\ell}} \cdot \overline{\mathbf{u}}_{\mathbf{q}, \ell}^{(2)} \right. \right. \right. \\ &\quad + \left(\frac{\mu_0}{\kappa_0^2} - \frac{\mu_\ell}{\kappa_\ell^2} \right) \text{div}_{\Gamma_{\mathbf{q}_\ell}} \left(\frac{1}{\mu_0} \mathbf{n}_{\mathbf{q}} \times \mathbf{curl} \overline{\mathbf{E}}_{\mathbf{q}, \bar{\mathbf{h}}} \right) \Big|_{\Gamma_{\mathbf{q}_\ell}} \cdot \text{div}_{\Gamma_{\mathbf{q}_\ell}} \overline{\mathbf{u}}_{\mathbf{q}, \ell}^{(2)} \\ &\quad - \left(\frac{\kappa_0^2}{\mu_0} - \frac{\kappa_\ell^2}{\mu_\ell} \right) \left(\mathbf{n}_{\mathbf{q}} \times \overline{\mathbf{E}}_{\mathbf{q}, \bar{\mathbf{h}}} \right) \Big|_{\Gamma_{\mathbf{q}_\ell}} \cdot \overline{\mathbf{u}}_{\mathbf{q}, \ell}^{(1)} \\ &\quad \left. \left. \left. + \left(\frac{1}{\mu_0} - \frac{1}{\mu_\ell} \right) \text{div}_{\Gamma_{\mathbf{q}_\ell}} \left(\mathbf{n}_{\mathbf{q}} \times \overline{\mathbf{E}}_{\mathbf{q}, \bar{\mathbf{h}}} \right) \Big|_{\Gamma_{\mathbf{q}_\ell}} \cdot \text{div}_{\Gamma_{\mathbf{q}_\ell}} \overline{\mathbf{u}}_{\mathbf{q}, \ell}^{(1)} \right\} \right) \circ \mathbf{q}_\ell \right]. \end{aligned}$$

Proof: The proof consists of three steps:

1. Factorisation of $F'[\mathbf{q}]$ and $F'[\mathbf{q}]^*$: Due to [Theorem 4](#) and [Remark 5](#) $F'[\mathbf{q}]$ has a factorisation

$$F'[\mathbf{q}]\boldsymbol{\xi} = \mathbf{A}^{\mathbf{q}}(\mathbf{B}^{\mathbf{q}_1} \boldsymbol{\xi}_1, \dots, \mathbf{B}^{\mathbf{q}_N} \boldsymbol{\xi}_N) \quad \text{where } \mathbf{B}^{\mathbf{q}_\ell} \boldsymbol{\xi}_\ell := \begin{bmatrix} \mathbf{B}_1^{\mathbf{q}_\ell} \boldsymbol{\xi}_\ell \\ \mathbf{B}_2^{\mathbf{q}_\ell} \boldsymbol{\xi}_\ell \end{bmatrix} := \begin{bmatrix} \mathbf{g}'_{\mathbf{q}_\ell, \boldsymbol{\xi}_\ell} \\ \mathbf{f}'_{\mathbf{q}_\ell, \boldsymbol{\xi}_\ell} \end{bmatrix}$$

with $\mathbf{f}'_{\mathbf{q}_\ell, \boldsymbol{\xi}_\ell}$ and $\mathbf{g}'_{\mathbf{q}_\ell, \boldsymbol{\xi}_\ell}$ defined in (28) and $\mathbf{A}^{\mathbf{q}}$ maps the boundary values $\begin{bmatrix} \mathbf{g}_{\mathbf{q}_\ell} \\ \mathbf{f}_{\mathbf{q}_\ell} \end{bmatrix}_{1 \leq \ell \leq N}$ onto the far-field pattern of the transmission problem (1a)–(14)–(1e) across the boundary $\Gamma_{\mathbf{q}}$, that is, $\mathbf{A}^{\mathbf{q}} := 2\mathbf{G}^{\mathbf{q}}(\mathbf{K}_{\text{IM}}^{\mathbf{q}})^{-1}$. Let us denote by $(\mathbf{A}^{\mathbf{q}})_{\mathbf{L}^2}^*$ and $(\mathbf{B}^{\mathbf{q}_\ell})_{\mathbf{L}^2}^*$ the adjoints of $\mathbf{A}^{\mathbf{q}}$ and $\mathbf{B}^{\mathbf{q}_\ell}$ with respect to the \mathbf{L}^2 inner products. ($\mathbf{B}^{\mathbf{q}_\ell}$ is unbounded and not everywhere defined from $\mathbf{L}^2(\Gamma_{\text{ref}}, \mathbb{R}^3)$ to $\mathbf{L}_t^2(\Gamma_{\mathbf{q}_\ell})^2$, but well-defined on $\mathbf{H}^1(\Gamma_{\text{ref}}, \mathbb{R}^3)$. Moreover, $\mathbf{B}^{\mathbf{q}}(\mathbf{H}^s(\Gamma_{\text{ref}}, \mathbb{R}^3)) \subset \mathbf{H}_{\text{div}}^{-1/2}(\Gamma_{\mathbf{q}_\ell})^2 \cap \mathbf{L}_t^2(\Gamma_{\mathbf{q}_\ell})^2$ for $s > 2$.) Therefore, the adjoint of $F'[\mathbf{q}]$ has the factorisation

$$F'[\mathbf{q}]^* \mathbf{h} = (\boldsymbol{\xi}_{\ell, \mathbf{h}}^*)_{1 \leq \ell \leq N} \quad \text{with } \boldsymbol{\xi}_{\ell, \mathbf{h}}^* = \mathbf{j}_{\mathcal{X} \hookrightarrow \mathbf{L}^2}^* (\mathbf{B}^{\mathbf{q}_\ell})_{\mathbf{L}^2}^* ((\mathbf{A}^{\mathbf{q}})_{\mathbf{L}^2}^* \mathbf{h}) \Big|_{\Gamma_{\mathbf{q}_\ell}},$$

and it remains to characterize $(\mathbf{A}^{\mathbf{q}})_{\mathbf{L}^2}^*$ and $(\mathbf{B}^{\mathbf{q}_\ell})_{\mathbf{L}^2}^*$.

2. Characterisation of $(\mathbf{A}^{\mathbf{q}})_{\mathbf{L}^2}^*$: Let us introduce the operator $\mathbf{G}_2^{\mathbf{q}} : \mathbf{L}_t^2(\Gamma_{\mathbf{q}}) \rightarrow \mathbf{L}_t^2(\mathbb{S}^2)$ by $(\mathbf{G}_2^{\mathbf{q}}\boldsymbol{\psi})(\hat{\mathbf{x}}) := \sum_{\ell=1}^N \frac{\mu_0}{4\pi} \hat{\mathbf{x}} \times \int_{\Gamma_{\mathbf{q}_\ell}} e^{-i\kappa_0 \hat{\mathbf{x}} \cdot \mathbf{y}} \boldsymbol{\psi}_\ell(\mathbf{y}) \, \mathrm{d}\mathbf{s}(\mathbf{y}) \times \hat{\mathbf{x}}$. Then

$$(\mathbf{G}_2^{\mathbf{q}})^* \mathbf{h} = ((\mathbf{G}_2^{\mathbf{q}_1})^* \mathbf{h}, \dots, (\mathbf{G}_2^{\mathbf{q}_N})^* \mathbf{h})$$

where

$$\begin{aligned} ((\mathbf{G}_2^{\mathbf{q}_\ell})^* \mathbf{h})(\mathbf{y}) &= \frac{\mu_0}{4\pi} \mathbf{n}_{\mathbf{q}_\ell}(\mathbf{y}) \times \left(\int_{\mathbb{S}^2} e^{i\kappa_0 \hat{\mathbf{x}} \cdot \mathbf{y}} \mathbf{h}(\hat{\mathbf{x}}) \, \mathrm{d}\mathbf{s}(\hat{\mathbf{x}}) \right)_{|\Gamma_{\mathbf{q}_\ell}} \times \mathbf{n}_{\mathbf{q}_\ell}(\mathbf{y}) \\ &= \mathbf{n}_{\mathbf{q}}(\mathbf{y}) \times \left(\overline{\mathbf{E}_{\mathbf{h}}^{\mathrm{inc}}} \right)_{|\Gamma_{\mathbf{q}_\ell}}(\mathbf{y}) \times \mathbf{n}_{\mathbf{q}}(\mathbf{y}). \end{aligned}$$

As $(\mathbf{G}^{\mathbf{q}_\ell} [\begin{smallmatrix} \boldsymbol{\varphi}_\ell \\ \boldsymbol{\psi}_\ell \end{smallmatrix}])(\hat{\mathbf{x}}) = \frac{i\kappa_0}{\mu_0} \hat{\mathbf{x}} \times (\mathbf{G}_2^{\mathbf{q}_\ell} \boldsymbol{\varphi}_\ell)(\hat{\mathbf{x}}) + (\mathbf{G}_2^{\mathbf{q}_\ell} \boldsymbol{\psi}_\ell)(\hat{\mathbf{x}})$ we obtain

$$(\mathbf{G}^{\mathbf{q}_\ell})_{\mathbf{L}^2}^* \mathbf{h} = \begin{bmatrix} \mathbf{n}_{\mathbf{q}_\ell} \times \left(\frac{1}{\mu_0} \mathbf{curl} \overline{\mathbf{E}_{\mathbf{h}}^{\mathrm{inc}}} \right)_{|\Gamma_{\mathbf{q}_\ell}} \times \mathbf{n}_{\mathbf{q}_\ell} \\ \mathbf{n}_{\mathbf{q}_\ell} \times \left(\overline{\mathbf{E}_{\mathbf{h}}^{\mathrm{inc}}} \right)_{|\Gamma_{\mathbf{q}_\ell}} \times \mathbf{n}_{\mathbf{q}_\ell} \end{bmatrix}.$$

Therefore, using [Remark 1](#) to pass from \mathbf{K}_{IM} to \mathbf{K}_{DM} , it follows that

$$\begin{aligned} \overline{(\mathbf{A}^{\mathbf{q}})_{\mathbf{L}^2}^* \mathbf{h}} &= \overline{((\mathbf{K}_{\mathrm{IM}}^{\mathbf{q}})^{-1})^* (\mathbf{G}^{\mathbf{q}})_{\mathbf{L}^2}^* \mathbf{h}} = 2(\mathbf{T}(\mathbf{K}_{\mathrm{IM}}^{\mathbf{q}}))^{-1} \overline{(\mathbf{G}^{\mathbf{q}})_{\mathbf{L}^2}^* \mathbf{h}} \\ &= \mathbf{R}^{\mathbf{q}}(\mathbf{K}_{\mathrm{DM}}^{\mathbf{q}})^{-1} \left[\begin{array}{c} 2\mathbf{E}_{\mathbf{h}}^{\mathrm{inc}}|_{\Gamma_{\mathbf{q}_\ell}} \times \mathbf{n}_{\mathbf{q}_\ell} \\ \frac{2}{\mu_0} \mathbf{curl} \mathbf{E}_{\mathbf{h}}^{\mathrm{inc}}|_{\Gamma_{\mathbf{q}_\ell}} \times \mathbf{n}_{\mathbf{q}_\ell} \end{array} \right]_{1 \leq \ell \leq N} \\ &= \left[\begin{array}{c} \mathbf{n}_{\mathbf{q}_\ell} \times \mathbf{E}_{\mathbf{q}, \bar{\mathbf{h}}|_{\Gamma_{\mathbf{q}_\ell}} \times \mathbf{n}_{\mathbf{q}_\ell} \\ \frac{1}{\mu_0} \mathbf{n}_{\mathbf{q}_\ell} \times \mathbf{curl} \mathbf{E}_{\mathbf{q}, \bar{\mathbf{h}}|_{\Gamma_{\mathbf{q}_\ell}} \times \mathbf{n}_{\mathbf{q}_\ell} \end{array} \right]_{1 \leq \ell \leq N} \end{aligned}$$

where we use [\(13\)](#) in the last line.

3. Characterisation of $(\mathbf{B}^{\mathbf{q}_\ell})_{\mathbf{L}^2}^*$: Compute $(\mathbf{B}^{\mathbf{q}_\ell})_{\mathbf{L}^2}^* \left[\begin{smallmatrix} \mathbf{g}_1 \times \mathbf{n}_{\mathbf{q}_\ell} \\ \mathbf{g}_2 \times \mathbf{n}_{\mathbf{q}_\ell} \end{smallmatrix} \right] = (\mathbf{B}_1^{\mathbf{q}_\ell})_{\mathbf{L}^2}^* (\mathbf{g}_1 \times \mathbf{n}_{\mathbf{q}_\ell}) + (\mathbf{B}_2^{\mathbf{q}_\ell})_{\mathbf{L}^2}^* (\mathbf{g}_2 \times \mathbf{n}_{\mathbf{q}_\ell})$. For $\mathbf{B}_1^{\mathbf{q}_\ell}$ using the integration by part for-

mula (39) we obtain

$$\begin{aligned} & \Re \langle \mathbf{g}_1 \times \mathbf{n}_{\mathbf{q}_\ell}, \mathbf{B}_1^{\mathbf{q}_\ell} \boldsymbol{\xi}_\ell \rangle_{\mathbf{L}_t^2(\Gamma_{\mathbf{q}_\ell})} \\ &= \int_{\Gamma_{\mathbf{q}_\ell}} (\boldsymbol{\xi}_\ell \circ \mathbf{q}_\ell^{-1} \cdot \mathbf{n}_{\mathbf{q}_\ell}) \Re \left\{ - \left(\frac{\kappa_0^2}{\mu_0} - \frac{\kappa_\ell^2}{\mu_\ell} \right) (\mathbf{g}_1 \times \mathbf{n}_{\mathbf{q}_\ell}) \cdot \left(\overline{\mathbf{u}_{\mathbf{q}_\ell}^{(1)}} \times \mathbf{n}_{\mathbf{q}_\ell} \right) \right. \\ & \quad \left. - \left(\frac{1}{\mu_0} - \frac{1}{\mu_\ell} \right) \operatorname{curl}_{\Gamma_{\mathbf{q}_\ell}} (\mathbf{g}_1 \times \mathbf{n}_{\mathbf{q}_\ell}) \cdot \operatorname{div}_{\Gamma_{\mathbf{q}_\ell}} \overline{\mathbf{u}_{\mathbf{q}_\ell}^{(1)}} \right\} ds. \end{aligned}$$

Together with the transformation formula $\int_{\Gamma_{\mathbf{q}_\ell}} f ds = \int_{\Gamma_{\text{ref}}} (f \circ \mathbf{q}_\ell) J_{\mathbf{q}_\ell} ds$ and the identities $(\mathbf{a} \times \mathbf{n}) \cdot (\mathbf{b} \times \mathbf{n}) = (\mathbf{n} \times \mathbf{a} \times \mathbf{n}) \cdot \mathbf{b}$ and (27) this yields

$$\begin{aligned} & (\mathbf{B}_1^{\mathbf{q}_\ell})_{\mathbf{L}^2}^* (\mathbf{g}_1 \times \mathbf{n}_{\mathbf{q}_\ell}) \\ &= J_{\mathbf{q}_\ell} \cdot \left(\mathbf{n}_{\mathbf{q}_\ell} \Re \left\{ - \left(\frac{\kappa_0^2}{\mu_0} - \frac{\kappa_\ell^2}{\mu_\ell} \right) (\mathbf{n}_{\mathbf{q}_\ell} \times \mathbf{g}_1 \times \mathbf{n}_{\mathbf{q}_\ell}) \cdot \overline{\mathbf{u}_{\mathbf{q}_\ell}^{(1)}} \right. \right. \\ & \quad \left. \left. + \left(\frac{1}{\mu_0} - \frac{1}{\mu_\ell} \right) \operatorname{div}_{\Gamma_{\mathbf{q}_\ell}} \mathbf{g}_1 \cdot \operatorname{div}_{\Gamma_{\mathbf{q}_\ell}} \overline{\mathbf{u}_{\mathbf{q}_\ell}^{(1)}} \right\} \right) \circ \mathbf{q}_\ell. \end{aligned}$$

Together with the analogous formula for $(\mathbf{B}_2^{\mathbf{q}_\ell})_{\mathbf{L}^2}^* (\mathbf{g}_2 \times \mathbf{n}_{\mathbf{q}_\ell})$ and parts 1 and 2 we obtain the assertion. ♠

Remark 7. In practice, the measurements are computed on a subset Γ_{obs} of \mathbb{S}^2 . Thus, we replace (29) by $\mathbf{E}_{\mathbf{h}}^{\text{inc}}(\mathbf{y}) := \frac{\mu_0}{4\pi} \int_{\Gamma_{\text{obs}}} e^{-i\kappa_0 \hat{\mathbf{x}} \cdot \mathbf{y}} \mathbf{h}(\hat{\mathbf{x}}) ds(\hat{\mathbf{x}})$, that we compute using the gauss quadrature formula [12, Eq. (2.42)] restricted to the gauss points located in Γ_{obs} .

Remark 8. Recall from the transformation formulas (19) that $(\operatorname{div}_{\Gamma_{\mathbf{q}_\ell}} \mathbf{v}) \circ \mathbf{q}_\ell = \frac{1}{J_{\mathbf{q}_\ell}} \operatorname{div}_{\mathbb{S}^2} (\mathcal{P}_{\mathbf{q}_\ell} \mathbf{v})$ and $\mathcal{P}_{\mathbf{q}_\ell} \operatorname{curl}_{\Gamma_{\mathbf{q}_\ell}} \mathbf{v} = \operatorname{curl}_{\mathbb{S}^2} (\mathbf{v} \circ \mathbf{q}_\ell)$. As both $\operatorname{div}_{\mathbb{S}^2}$ and $\operatorname{curl}_{\mathbb{S}^2}$ are diagonal with respect to the chosen bases of spherical harmonics and vector spherical harmonics, the implementation of the formulas in Remark 5 and Proposition 6 is straightforward using our discretisation.

Using [22, Corollary 4] we obtain that $\mathbf{F}'_{\text{star}}[\mathbf{r}]^* \mathbf{h} = (\mathbf{j}_{\mathcal{X}_{\text{star}} \hookrightarrow \mathbf{L}^2} \mathbf{r}_\ell^2 \Re \{ \cdots \} \circ \mathbf{q}_\ell)_{1 \leq \ell \leq N}$ where the expression in the curly brackets coincides with that in Proposition 6.

7 Implementation of the Newton method and numerical examples

For any $\mathbf{n} \in \mathbb{N}^*$, let $\mathbb{H}_{\mathbf{n}}^{\mathbb{R}}$ be the $(\mathbf{n} + 1)^2$ dimensional space spanned by the orthonormal scalar real spherical harmonics of degree at most \mathbf{n} . In the sequel, we consider that the unknown radial parametrisations $\mathbf{q}_{\delta}^k = (\mathbf{q}_{\ell, \delta}^k = \mathbf{c}_{\ell} + \mathcal{R}r_{\ell, \delta}^k)_{1 \leq \ell \leq \mathbf{N}}$ are approached by scalar spherical harmonics of degree at most \mathbf{n}_{star} , respectively, that means $r_{\ell, \delta}^k \in \mathbb{H}_{\mathbf{n}_{\text{star}}}^{\mathbb{R}}$. The far-field data are evaluated at some quadrature points $\hat{\mathbf{x}}_{\text{obs}}^s = (\hat{\mathbf{x}}_1^s, \hat{\mathbf{x}}_2^s, \hat{\mathbf{x}}_3^s) = (\cos \phi_r \sin \theta_s, \sin \phi_r \sin \theta_s, \cos \theta_s)$ with $\theta_s = \cos^{-1} z_s$, where z_s , for $s = 1, \dots, \mathbf{n}_{\text{meas}} + 1$, are the zeros of the Legendre polynomial of degree $\mathbf{n}_{\text{meas}} + 1$, and $\phi_r = \frac{r\pi}{\mathbf{n}_{\text{meas}} + 1}$, for $r = 0, \dots, 2\mathbf{n}_{\text{meas}} + 1$. Let us summarize the numerical implementation of the k th regularised Newton step for the operator equation (22):

1. In the parametrisation of the current reconstruction $\Gamma_{\delta}^k := \bigcup_{\ell=1}^{\mathbf{N}} \mathbf{q}_{\ell, \delta}^k(\Gamma_{\text{ref}})$, evaluate the forward operator \mathbf{F} by solving the discretized approximation of the integral equation (13) of the direct method $\mathbf{K}_{\text{DM}}(\mathbf{u}_{\ell}^{(j)})_{1 \leq \ell \leq \mathbf{N}} = 2(\mathbf{u}_{\ell}^{\text{inc}, j})_{1 \leq \ell \leq \mathbf{N}}$ for all incident waves $j = 1, \dots, \mathbf{m}$ using an LU decomposition of the matrix \mathbf{K}_{DM} . Save the Fourier coefficients of $\mathbf{u}^{(j)}$ of the total exterior fields $(\mathbf{n} \times (\mathbf{E}^{\text{s}, j} + \mathbf{E}^{\text{inc}, j}), \mathbf{n} \times \text{curl}(\mathbf{E}^{\text{s}, j} + \mathbf{E}^{\text{inc}, j}))^{\top}$ on Γ_{δ}^k . Finally compute the discrete far-field patterns $\mathbf{E}^{\infty, j} = \sum_{\ell=1}^{\mathbf{N}} \mathbf{G}^{\ell} \mathbf{u}_{\ell}^{(j)}$ for the j th incident wave and the interface Γ_{δ}^k .
2. Now $\mathbf{F}'[\mathbf{q}_{\delta}^k] \boldsymbol{\xi}$ is evaluated for any $\boldsymbol{\xi}$ by solving discretised versions of the integral equation (16) $\mathbf{K}_{\text{IM}}(\boldsymbol{\psi}_{\ell}^{(j)}, \boldsymbol{\varphi}_{\ell}^{(j)})_{1 \leq \ell \leq \mathbf{N}} = 2(\mathbf{g}_{\mathbf{q}_{\ell, \delta}^k, \xi_{\ell}}^{(j)'}, \mathbf{f}_{\mathbf{q}_{\ell, \delta}^k, \xi_{\ell}}^{(j)'})_{1 \leq \ell \leq \mathbf{N}}$ for $j = 1, \dots, \mathbf{m}$. The right hand sides are evaluated using the solutions $\mathbf{u}^{(j)}$ from point 1 (see Remark 8). For the inversion of the matrix \mathbf{K}_{IM} the LU-decomposition of \mathbf{K}_{DM} is reused (see Remark 1). Finally, $\mathbf{F}'[\mathbf{q}_{\delta}^k] \boldsymbol{\xi}$ is approximated by the concatenation of the vectors $\sum_{\ell=1}^{\mathbf{N}} \mathbf{G}^{\ell}(\boldsymbol{\psi}_{\ell}^{(j)}, \boldsymbol{\varphi}_{\ell}^{(j)})$ for $j = 1, \dots, \mathbf{m}$.

Similarly, to compute $F'[\mathbf{q}_\delta^k]^* \mathbf{h}$ with $\mathbf{h} = (\mathbf{h}^{(1)}, \dots, \mathbf{h}^{(m)})$, we compute traces of the total fields $\mathbf{E}_{\mathbf{q}_\delta^k, \overline{\mathbf{h}^{(j)}}}$ for Herglotz incident fields with kernels $\overline{\mathbf{h}^{(j)}}$ by evaluating $2\mathbf{K}_{\text{IM}}^\top(\mathbf{G}^{\ell^\top} \overline{\mathbf{h}^{(j)}})_{1 \leq \ell \leq N}$. Then we use the formula in Proposition 6 and sum up the results for each j to obtain $F'[\mathbf{q}_\delta^k]^* \mathbf{h}$.

3. Compute the next iterate \mathbf{q}_δ^{k+1} by minimizing the quadratic Tikhonov functional (23) (or solving the equivalent linear equation (24)) by the conjugate gradient method. In each conjugate gradient step $F'[\mathbf{q}_\delta^k]$ and $F'[\mathbf{q}_\delta^k]^*$ are applied to some vectors as described in point 2.

In the conjugate gradient algorithm we only compute L^2 adjoint $F'[\mathbf{q}_\delta^k]^*_{L^2}$ and evaluate norms in $\mathcal{X} = H^s(\mathbb{S}^2)$ using Proposition 9 and norms in $\mathcal{Y} = L^2_t(\Gamma_{\text{obs}})^m$ using a quadrature formula. For more practical uses of the inverse algorithm combined with boundary element methods, the computation of integrals over Γ_{obs} for evaluating either the Herglotz incident fields or norms in \mathcal{Y} can be replaced by a discrete sum over an equidistributed sequence of points in Γ_{obs} .

Our numerical experiments are concerned with the shape reconstruction of the obstacles described in Table 1, see Figure 1(a) or Figure 2(a). We solve, using first order linearisation of the far-field operator, the inverse problem equation (22) at a finite set of observation directions dispersed either on the far-field sphere $\Gamma_{\text{obs}} = \mathbb{S}^2$ (that is using full-scattering noisy data) or on the far-field half-sphere $\Gamma_{\text{obs}} = \mathbb{S}^2 \cap \{\hat{\mathbf{x}}_2 \geq 0\}$ (that is using back-scattering noisy data) or on the far-field half-sphere $\Gamma_{\text{obs}} = \mathbb{S}^2 \cap \{\hat{\mathbf{x}}_2 \leq 0\}$ (that is using forward-scattering noisy data). In all experiments, we use $n_{\text{meas}} = 7$ and compute the far-field data at the gauss quadrature points $\hat{\mathbf{x}}_{\text{obs}}^s \in \Gamma_{\text{obs}}$ for evaluating the Herglotz incident fields (29).

As a first test, we iteratively recover the shape of four dielectric scatterers illuminated by five incident plane waves coming from the half-space $\hat{\mathbf{x}}_2 \geq 0$

that are defined by the following directions and polarisations:

$$\begin{aligned}\mathbf{d}_1 &= (0, -1, 0), & \mathbf{d}_2 &= (0, -\frac{\sqrt{2}}{2}, \frac{\sqrt{2}}{2}), & \mathbf{d}_3 &= (0, -\frac{\sqrt{2}}{2}, -\frac{\sqrt{2}}{2}), \\ \mathbf{d}_4 &= (\frac{\sqrt{2}}{2}, -\frac{\sqrt{2}}{2}, 0), & \mathbf{d}_5 &= (-\frac{\sqrt{2}}{2}, -\frac{\sqrt{2}}{2}, 0) \\ \mathbf{p}_1 &= \mathbf{p}_2 = \mathbf{p}_3 = (1, 0, 0), & \mathbf{p}_4 &= \mathbf{p}_5 = (0, 0, 1).\end{aligned}$$

We consider back-scattering measurements with random noise level of 1% in [Figure 1\(b\)](#), forward-scattering measurements with random noise level of 1% (c) and back-scattering measurements with random noise level of 5% in [Figure 1\(d\)](#). The exterior parameters are $\mu_0 = 1$ and $\kappa_0 = \pi$ so that the diameters of the scatterers are roughly 0.5ℓ or 0.6ℓ . The separation distance between the obstacles varies between 0.5ℓ or 1.5ℓ . To compute the exact far-field data we use $\mathbf{n} = 15$ for the four obstacles. To compute the far-field data at each iteration step we use $\mathbf{n} = 10$. The radial functions describing the unknown parametrisation belong to $\mathbb{H}_{15}^{\mathbb{R}}$. The initial guesses are four spheres with diameters 0.6ℓ located at the already known centers given in [Table 1](#). Using the discrepancy principle, the algorithm is stopped at the first index k for which

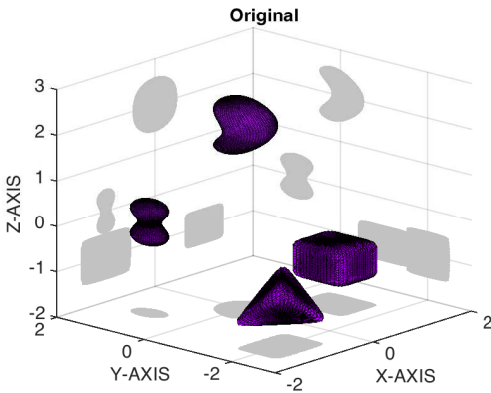
$$\|F(\mathbf{q}_\delta^k) - \mathbf{E}_\delta^\infty\| \leq \tau\delta \quad (30)$$

where we choose $\tau = 1.5$. We set $\alpha_0 = 0.1$. The numerical experiments were realised on a laptop with a 2.7 GHz processor with four workers and 8 GB RAM. The CPU time for one iteration is about 25 min. With this stopping rule we obtain the picture presented in [Figure 1\(b\)](#) after 17 iterations, the picture presented in [Figure 1\(c\)](#) after 13 iterations, and the picture presented in [Figure 1\(d\)](#) after 10 iterations. As a result, we find that we obtain similar partial reconstruction using either forward- or back-scattering measurements. By increasing the degree of spherical harmonics describing the shapes (i.e., with $\mathbf{n} \geq 30$), one can even recover the sharp angle of the rectangle and the tetrahedron. Also as expected, the low contrast between exterior and interior parameters renders the shape reconstruction of the peanut rather difficult.

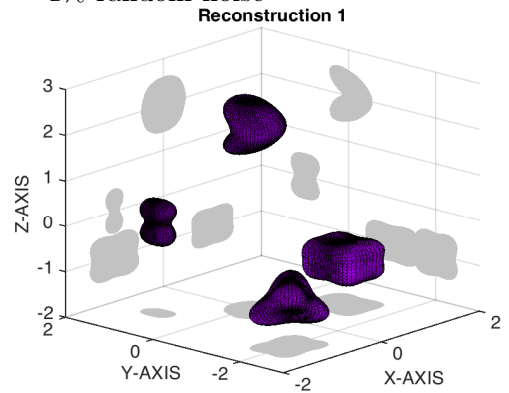
As a second test, we analyze the influence of the number of incident plane waves. We iteratively recover the shape of two identical obstacles illuminated

Figure 1: Iterative shape reconstruction of four dielectric obstacles illuminated by 5 incoming plane waves from the half-space $\hat{\mathbf{x}}_2 \geq 0$: (b-c) $\kappa_\ell = 2\kappa_0$, $\mu_\ell = \mu_0$ for $1 \leq \ell \leq 4$, and (d) $\kappa_1 = 1.2\kappa_0$, $\kappa_2 = 2\kappa_0$, $\kappa_3 = 1.5\kappa_0$, $\kappa_4 = 0.7\kappa_0$, $\mu_1 = \mu_0$, $\mu_2 = 1.1\mu_0$, $\mu_3 = 0.9\mu_0$, $\mu_4 = 1.5\mu_0$. Click on an image to download a movie of the iterations.

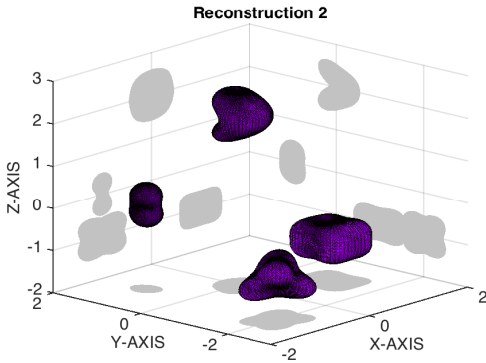
(a) $\Gamma = \Gamma_1 \cup \Gamma_2 \cup \Gamma_3 \cup \Gamma_4$



(b) back-scattering data with 1% random noise



(c) forward-scattering data with 1% random noise



(d) back-scattering data with 5% random noise

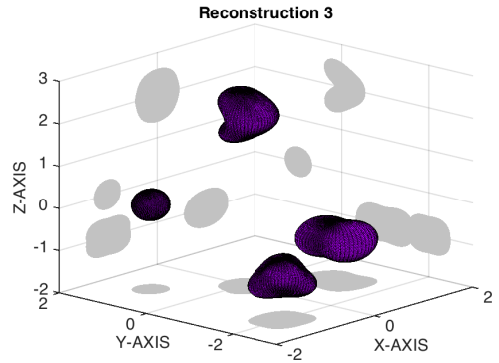
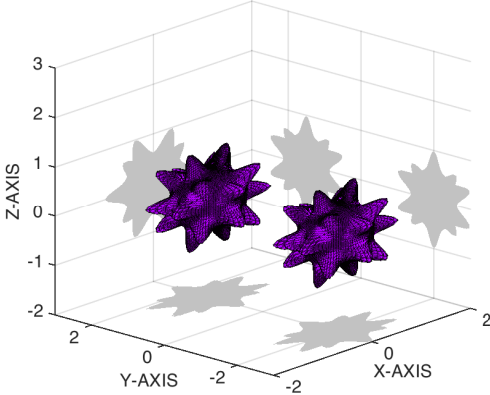


Figure 2: Iterative shape reconstruction of two identical dielectric obstacles illuminated by either one or several incident plane waves coming from the half-space $\hat{x}_2 \geq 0$ and with 5% noise. Click on an image to download a movie of the iterations.

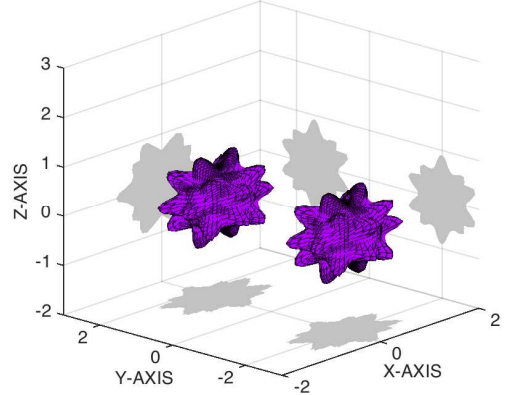
(a) $\Gamma = \{(0, 1.5, 0) + \Gamma_5\} \cup \{(0, -2, 0) + \Gamma_5\}$

Original



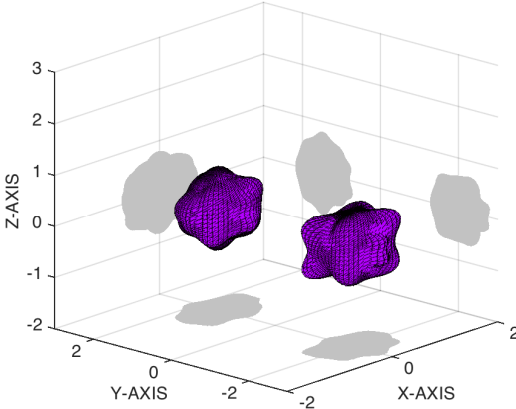
(b) five incoming plane waves

Reconstruction 1



(c) one incoming plane wave

Reconstruction 2



either by one incident plane wave defined by the couple $(\mathbf{d}_1, \mathbf{p}_1)$ in Figure 2(b) or by the five incident plane waves above defined in Figure 2(c). The geometry of the obstacles requires a higher frequency and in our experiments we set $\kappa_0 = 2\pi$ so that the diameters of the scatterers are roughly $2l$. The interior parameters are $\kappa_\ell = 2\kappa_0$ and $\mu_\ell = \mu_0$. The separation distance between the obstacles is about $1.5l$. To compute the exact far-field data we use $\mathbf{n} = 25$ for the four obstacles. To compute the far-field data at each iteration step we use $\mathbf{n} = 20$. The radial functions describing the unknown parametrisation belong to $\mathbb{H}_{20}^{\mathbb{R}}$. We use either back-scattering measurements in Figure 2(b) or full-scattering measurements in Figure 2(c) with a random noise level of 5%. With the stopping rule (30) and $\tau = 1.5$, we obtain the picture presented in Figure 2(b) after 26 iterations and the picture presented in Figure 2(c) after 17 iterations. As a result we find that collecting the far-field data in all directions for a single incident wave is not sufficient to recover the 20 peaks of the stellated dodecahedron. Using partial far-field measurements and increasing the number of incident plane waves, we obtain very accurate reconstruction of the dielectric obstacles, even for the one located in the shadow part.

8 Conclusion

This paper demonstrates that Gauss–Newton iterative method applied to the first order linearisation of the objective functional F is a powerful tool for solving 3D inverse multiple scattering problems, provided that a fast solver is used to evaluate F . Increasing the number of obstacles, we suggest using the indirect solver [18]. Incomplete knowledge of the scattered data corresponding to very few incident waves suffices to recover an accurate approximation of the shape of the multiple obstacles by opposition to sampling methods [5]. The main drawback is that we need to know from the beginning the exact number of obstacles, their size and location. The latter issue can be handled by combining the iterative algorithm to qualitative methods such

as topological gradient based method [6] or T-matrix based method [48]. The domain-derivative based formulation in the Gauss–Newton iterations can also be replaced by the material-derivative based formulation [31] that avoids the solution of the forward problem in the nonlinear least square. The analysis and comparison of the resulting hybrid methods for more complicated configurations (multiple-layered media) is the subject of future work.

A Surface differential operators

First we briefly recall the definitions and some properties of surface differential operators [43]. Assuming that Γ admits an atlas $(\Gamma_i, \mathcal{O}_i, \psi_i)_{1 \leq i \leq p}$, where $(\Gamma_i)_{1 \leq i \leq p}$ is a covering of open subset of Γ and for $i = 1, \dots, p$, the function ψ_i is a diffeomorphism (of class \mathcal{C}^1 at least) such that $\psi_i^{-1}(\Gamma_i) = \mathcal{O}_i \subset \mathbb{R}^2$, then when $\mathbf{x} \in \Gamma_i$ we write $\mathbf{x} = \psi_i(\xi_1^x, \xi_2^x)$ where $(\xi_1^x, \xi_2^x) \in \mathcal{O}_i$. The tangent plane to Γ at \mathbf{x} is generated by the vectors

$$\mathbf{e}_1(\mathbf{x}) = \frac{\partial \psi_i}{\partial \xi_1}(\xi_1^x, \xi_2^x) \quad \text{and} \quad \mathbf{e}_2(\mathbf{x}) = \frac{\partial \psi_i}{\partial \xi_2}(\xi_1^x, \xi_2^x).$$

The unit outer normal vector to Γ and the surface area element are

$$\mathbf{n} = \frac{\mathbf{e}_1 \times \mathbf{e}_2}{|\mathbf{e}_1 \times \mathbf{e}_2|} \quad \text{and} \quad ds(\mathbf{y}) = |\mathbf{e}_1(\mathbf{y}) \times \mathbf{e}_2(\mathbf{y})| d\xi_1 d\xi_2 = J_{\psi_i}(\mathbf{y}) d\xi_1 d\xi_2,$$

where J_{ψ_i} denotes the determinant of the Jacobian matrix of $\psi_i : \mathcal{O}_i \mapsto \Gamma_i$. The cotangent plane to Γ at \mathbf{x} is generated by the vectors

$$\mathbf{e}^1(\mathbf{x}) = \frac{\mathbf{e}_2(\mathbf{x}) \times \mathbf{n}(\mathbf{x})}{J_{\psi_i}(\mathbf{x})} \quad \text{and} \quad \mathbf{e}^2(\mathbf{x}) = \frac{\mathbf{n}(\mathbf{x}) \times \mathbf{e}_1(\mathbf{x})}{J_{\psi_i}(\mathbf{x})}.$$

For $i = 1, 2$, $\mathbf{e}_i \cdot \mathbf{e}^j = \delta_i^j$ where δ_i^j represents the Kronecker symbol.

The tangential gradient and the tangential vector curl of any scalar function $\mathbf{u} \in \mathcal{C}^1(\Gamma, \mathbb{C})$ are defined for $\mathbf{x} = \psi_i(\xi_1^x, \xi_2^x) \in \Gamma$ by

$$\text{grad}_\Gamma \mathbf{u}(\mathbf{x}) = \frac{\partial(\mathbf{u} \circ \psi_i)}{\partial \xi_1} \circ \psi_i^{-1}(\mathbf{x}) \mathbf{e}^1(\mathbf{x}) + \frac{\partial(\mathbf{u} \circ \psi_i)}{\partial \xi_2} \circ \psi_i^{-1}(\mathbf{x}) \mathbf{e}^2(\mathbf{x}), \quad (31)$$

$$\mathbf{curl}_\Gamma \mathbf{u}(\mathbf{x}) = \frac{1}{J_{\psi_i}(\mathbf{x})} \left[\frac{\partial(\mathbf{u} \circ \psi_i)}{\partial \xi_2} \circ \psi_i^{-1}(\mathbf{x}) \mathbf{e}_1(\mathbf{x}) - \frac{\partial(\mathbf{u} \circ \psi_i)}{\partial \xi_1} \circ \psi_i^{-1}(\mathbf{x}) \mathbf{e}_2(\mathbf{x}) \right]. \quad (32)$$

such that $\text{grad}_\Gamma \mathbf{u} = (\text{grad } \tilde{\mathbf{u}})|_\Gamma$ and $\mathbf{curl}_\Gamma \mathbf{u} = \mathbf{curl}(\tilde{\mathbf{u}}\tilde{\mathbf{n}})|_\Gamma$ for any smooth extension $\tilde{\mathbf{u}}$ of \mathbf{u} to a neighborhood of Γ and a smooth extension $\tilde{\mathbf{n}}$ of \mathbf{n} as gradient of a distance function. Moreover, define the surface divergence of any vector function $\mathbf{v} = v^1 \mathbf{e}_1 + v^2 \mathbf{e}_2 \in \mathcal{C}^1(\Gamma, \mathbb{C}^3)$ in the tangent plane to Γ and the surface scalar curl of any vector function $\mathbf{w} = w_1 \mathbf{e}^1 + w_2 \mathbf{e}^2 \in \mathcal{C}^1(\Gamma, \mathbb{C}^3)$ in the cotangent plane to Γ or $\mathbf{x} = \psi_i(\xi_1^x, \xi_2^x) \in \Gamma$ by

$$\text{div}_\Gamma \mathbf{v}(\mathbf{x}) = \frac{1}{J_{\psi_i}(\mathbf{x})} \left(\frac{\partial(J_{\psi_i} v^1) \circ \psi_i}{\partial \xi_1} + \frac{\partial(J_{\psi_i} v^2) \circ \psi_i}{\partial \xi_2} \right) \circ \psi_i^{-1}(\mathbf{x}), \quad (33)$$

$$\text{curl}_\Gamma \mathbf{w}(\mathbf{x}) = \frac{1}{J_{\psi_i}(\mathbf{x})} \left(\frac{\partial(w_2 \circ \psi_i)}{\partial \xi_1} - \frac{\partial(w_1 \circ \psi_i)}{\partial \xi_2} \right) \circ \psi_i^{-1}(\mathbf{x}). \quad (34)$$

These definitions are independent of the choice of the coordinate system, and the identities

$$\mathbf{n} \cdot (\mathbf{curl} \mathbf{E})|_\Gamma = \text{curl}_\Gamma(\mathbf{n} \times \mathbf{E} \times \mathbf{n}), \quad (35)$$

$$\mathbf{curl}_\Gamma \mathbf{u} = (\text{grad}_\Gamma \mathbf{u}) \times \mathbf{n}, \quad \text{curl}_\Gamma(\mathbf{w}) = \text{div}_\Gamma(\mathbf{w} \times \mathbf{n}), \quad (36)$$

$$\text{curl}_\Gamma \text{grad}_\Gamma \mathbf{u} = 0, \quad \text{div}_\Gamma \mathbf{curl}_\Gamma \mathbf{u} = 0, \quad (37)$$

hold for \mathbf{u} and \mathbf{w} and any smooth vector function \mathbf{E} defined on a neighborhood of Γ . By density arguments, the surface differential operators can be extended to Sobolev spaces. For $s \in \mathbb{R}$, $\boldsymbol{\varphi} \in \mathbf{H}_t^{s+1}(\Gamma)$ and $\boldsymbol{\varphi} \in \mathbf{H}^{-s}(\Gamma)$ we have the

dualities

$$\int_{\Gamma} (\operatorname{div}_{\Gamma} \boldsymbol{\varphi}) \cdot \boldsymbol{\varphi} \, ds = - \int_{\Gamma} \boldsymbol{\varphi} \cdot \operatorname{grad}_{\Gamma} \boldsymbol{\varphi} \, ds, \quad (38)$$

$$\int_{\Gamma} (\operatorname{curl}_{\Gamma} \boldsymbol{\varphi}) \cdot \boldsymbol{\varphi} \, ds = \int_{\Gamma} \boldsymbol{\varphi} \cdot \operatorname{curl}_{\Gamma} \boldsymbol{\varphi} \, ds. \quad (39)$$

B Spherical harmonics and Sobolev spaces on \mathbb{S}^2

In this appendix we recall the characterisations of Sobolev spaces on \mathbb{S}^2 by scalar and vector spherical harmonics [43]. For $l \in \mathbb{N}$ and $0 \leq j \leq l$, let P_l^j denote the j th associated Legendre function of order l (provided by MATLAB). Using the notation (18), the spherical harmonics are defined by

$$Y_{l,j}(\hat{\mathbf{x}}) = (-1)^{(|j|-j)/2} \sqrt{\frac{2l+1}{4\pi} \frac{(l-|j|!)}{(l+|j|!)}} P_l^{|j|}(\cos \theta) e^{ij\phi}$$

for $j = -l, \dots, l$ and $l = 0, 1, 2, \dots$

Proposition 9. $\{Y_{l,j} : l, j \in \mathbb{Z}, l \geq 0, |j| \leq l\}$ is a complete orthonormal system in $L^2(\mathbb{S}^2)$. The complex Hilbert spaces $H^s(\mathbb{S}^2)$ for $s \in \mathbb{R}$ can be characterized by

$$H^s(\mathbb{S}^2) = \left\{ \mathbf{q} = \sum_{l=0}^{\infty} \sum_{j=-l}^l c_{l,j} Y_{l,j} : c_{l,j} \in \mathbb{C} \text{ and } \sum_{l=1}^{\infty} \sum_{j=-l}^l (1+l^2)^s |c_{l,j}|^2 < +\infty \right\},$$

with (equivalent) norm $\|\mathbf{q}\|_{H^s}^2 = \sum_{l=1}^{\infty} \sum_{j=-l}^l (1+l^2)^s |c_{l,j}|^2 = \sum_{l=1}^{\infty} \sum_{j=-l}^l (1+l^2)^s \left| \int_{\mathbb{S}^2} \mathbf{q} \cdot \overline{Y_{l,j}} \, ds \right|^2$. A function $\mathbf{q} \in H^s(\mathbb{S}^2, \mathbb{C})$ is real valued if and only if $c_{l,-j} = (-1)^j \overline{c_{l,j}}$ for all $l = 0, 1, \dots$ and $j = -l, \dots, l$.

The tangential gradient of the spherical harmonics is

$$\begin{aligned} & \text{grad}_{\mathbb{S}^2} Y_{\mathfrak{l},j}(\hat{\mathbf{x}}) \\ &= \begin{cases} (-1)^{(|j|-j)/2} \sqrt{\frac{2\mathfrak{l}+1}{4\pi} \frac{(\mathfrak{l}-|j|!)}{(\mathfrak{l}+|j|)!}} \left(\frac{\partial P_{\mathfrak{l}}^{j|j|}(\cos \theta)}{\partial \theta} \mathbf{e}_{ij\phi} \mathbf{e}_{\theta} + ij \frac{P_{\mathfrak{l}}^{j|j|}(\cos \theta)}{\sin \theta} \mathbf{e}_{ij\phi} \mathbf{e}_{\phi} \right), \\ \quad \sin \theta \neq 0, \\ -(-1)^{(|j|-j)/2} \sqrt{\mathfrak{l}(\mathfrak{l}+1) \frac{2\mathfrak{l}+1}{4\pi}} \left(\frac{(\cos \theta)^{\mathfrak{l}}}{2} \mathbf{e}_{\theta} + ij \frac{(\cos \theta)^{\mathfrak{l}+1}}{2} \mathbf{e}_{\phi} \right), \\ \quad \sin \theta = 0, |j| = 1; \\ (0, 0, 0), \quad \sin \theta = 0, |j| \neq 1; \end{cases} \end{aligned}$$

for $\mathfrak{l} \in \mathbb{N}^*$ and $j \in \mathbb{N}$ with $|j| \leq \mathfrak{l}$ with

$$\frac{\partial P_{\mathfrak{l}}^{j|j|}(\cos \theta)}{\partial \theta} = \begin{cases} -(\mathfrak{l} + |j|)(\mathfrak{l} - |j| + 1) P_{\mathfrak{l}}^{j|j|-1}(\cos \theta) - |j| \frac{\cos \theta}{\sin \theta} P_{\mathfrak{l}}^{j|j|}(\cos \theta), \\ \quad |j| \neq 0; \\ P_{\mathfrak{l}}^1(\cos \theta), \quad \text{otherwise.} \end{cases}$$

The tangential vector spherical harmonics are defined by

$$\mathbf{y}_{\mathfrak{l},j}^{(1)} = \frac{1}{\sqrt{\mathfrak{l}(\mathfrak{l}+1)}} \text{grad}_{\mathbb{S}^2} Y_{\mathfrak{l},j} \quad \text{and} \quad \mathbf{y}_{\mathfrak{l},j}^{(2)} = \frac{1}{\sqrt{\mathfrak{l}(\mathfrak{l}+1)}} \text{curl}_{\mathbb{S}^2} Y_{\mathfrak{l},j}$$

for $j = -\mathfrak{l}, \dots, \mathfrak{l}$ and $\mathfrak{l} = 1, 2, \dots$ and form a complete orthonormal system in $\mathbf{L}_t^2(\mathbb{S}^2)$.

Acknowledgments I thank Olha Ivanyshyn Yaman for providing the MATLAB code of the acoustic operators [12] and visualisation tools developed [30] that has been extended to the electromagnetic case [16, 17] in this work. Thorsten Hohage is gratefully acknowledged for providing the inversion toolbox he developed with MATLAB programming language [27, 28] and for helpful discussions. Part of this work was carried out under the financial support of DFG through CRC 755 at the University of Goettingen.

References

- [1] A. Altundag, *On a Two-Dimensional Inverse Scattering Problem for a Dielectric*, PhD thesis, University of Göttingen, 2012. [E6](#)
- [2] K. E. Atkinson, The numerical solution of Laplace's equation in three dimensions, *SIAM J. Numer. Anal.*, 19 (1982), pp. 263–274. doi:[10.1137/0719017](#) [E7](#)
- [3] A. B. Bakushinskiĭ, On a convergence problem of the iterative-regularized Gauss–Newton method, *Comput. Math. Math. Phys.*, 32 (1992), pp. 1503–1509. [E6](#)
- [4] A. Buffa, R. Hiptmair, T. von Petersdorff, and C. Schwab, Boundary element methods for Maxwell transmission problems in Lipschitz domains, *Numer. Math.*, 95 (2003), pp. 459–485. doi:[10.1007/s00211-002-0407-z](#) [E4](#)
- [5] F. Cakoni, D. Colton, and P. Monk, *The linear sampling method in inverse electromagnetic scattering*, vol. 80 of CBMS-NSF Regional Conference Series in Applied Mathematics, Society for Industrial and Applied Mathematics, Philadelphia, PA, 2011. [E39](#)
- [6] A. Carpio, B. T. Johansson, and M.-L. Rapún, Determining planar multiple sound-soft obstacles from scattered acoustic fields, *J. Math. Imaging Vision*, 36 (2010), pp. 185–199. doi:[10.1007/s10851-009-0182-x](#) [E40](#)
- [7] D. Colton and R. Kress, *Inverse acoustic and electromagnetic scattering theory*, vol. 93 of Applied Mathematical Sciences, Springer, New York, third ed., 2013. [E5](#)
- [8] M. Costabel and F. Le Louër, On the Kleinman–Martin integral equation method for electromagnetic scattering by a dielectric body, *SIAM J. Appl. Math.*, 71 (2011), pp. 635–656. doi:[10.1137/090779462](#) [E5](#), [E6](#)

- [9] M. Costabel and F. Le Louër, Shape derivatives of boundary integral operators in electromagnetic scattering. Part I: Shape differentiability of pseudo-homogeneous boundary integral operators, *Integr. Equ. Oper. Theory*, 72 (2012), pp. 509–535. doi:[10.1007/s00020-012-1954-z](https://doi.org/10.1007/s00020-012-1954-z) E6
- [10] M. Costabel and F. Le Louër, Shape derivatives of boundary integral operators in electromagnetic scattering. Part II: Application to scattering by a homogeneous dielectric obstacle, *Integr. Equ. Oper. Theory*, 73 (2012), pp. 17–48. doi:[10.1007/s00020-012-1955-y](https://doi.org/10.1007/s00020-012-1955-y) E6, E17, E28
- [11] A. de La Bourdonnaye, Décomposition de $H_{\text{div}}^{-1/2}(\Gamma)$ et nature de l’opérateur de Steklov–Poincaré du problème extérieur de l’électromagnétisme, *C. R. Acad. Sci. Paris Sér. I Math.*, 316 (1993), pp. 369–372. E16
- [12] M. Ganesh and I. G. Graham, A high-order algorithm for obstacle scattering in three dimensions, *J. Comput. Phys.*, 198 (2004), pp. 211–242. doi:[10.1016/j.jcp.2004.01.007](https://doi.org/10.1016/j.jcp.2004.01.007) E7, E19, E22, E23, E33, E43
- [13] M. Ganesh and S. C. Hawkins, A spectrally accurate algorithm for electromagnetic scattering in three dimensions, *Numer. Algorithms*, 43 (2006), pp. 25–60. doi:[10.1007/s11075-006-9033-7](https://doi.org/10.1007/s11075-006-9033-7) E7
- [14] M. Ganesh and S. C. Hawkins, An efficient surface integral equation method for the time-harmonic Maxwell equations, *ANZIAM J.*, 48 (2007), pp. C17–C33. doi:[10.21914/anziamj.v48i0.60](https://doi.org/10.21914/anziamj.v48i0.60) E7
- [15] M. Ganesh and S. C. Hawkins, A hybrid high-order algorithm for radar cross section computations, *SIAM J. Sci. Comput.*, 29 (2007), pp. 1217–1243. doi:[10.1137/060664859](https://doi.org/10.1137/060664859) E7, E20
- [16] M. Ganesh and S. C. Hawkins, A high-order tangential basis algorithm for electromagnetic scattering by curved surfaces, *J. Comput. Phys.*, 227 (2008), pp. 4543–4562. doi:[10.1016/j.jcp.2008.01.016](https://doi.org/10.1016/j.jcp.2008.01.016) E7, E19, E20, E43

- [17] M. Ganesh and S. C. Hawkins, A high-order algorithm for multiple electromagnetic scattering in three dimensions, *Numer. Algorithms*, 50 (2009), pp. 469–510. doi:[10.1007/s11075-008-9238-z](https://doi.org/10.1007/s11075-008-9238-z) E7, E43
- [18] M. Ganesh and S. C. Hawkins, An efficient $O(N)$ algorithm for computing $O(N^2)$ acoustic wave interactions in large N -obstacle three dimensional configurations, *BIT*, 55 (2015), pp. 117–139. doi:[10.1007/s10543-014-0491-3](https://doi.org/10.1007/s10543-014-0491-3) E39
- [19] M. Ganesh, S. C. Hawkins and D. Volkov, An all-frequency weakly-singular surface integral equation for electromagnetism in dielectric media: Reformulation and well-posedness analysis, *J. Math. Anal. Appl.*, 412 (2014), pp. 277–300. doi:[10.1016/j.jmaa.2013.10.059](https://doi.org/10.1016/j.jmaa.2013.10.059) E5, E7
- [20] H. Haddar and R. Kress, On the Fréchet derivative for obstacle scattering with an impedance boundary condition, *SIAM J. Appl. Math.*, 65 (2004), pp. 194–208 (electronic). doi:[10.1137/S0036139903435413](https://doi.org/10.1137/S0036139903435413) E6
- [21] P. Hähner, A uniqueness theorem for a transmission problem in inverse electromagnetic scattering, *Inverse Problems*, 9 (1993), pp. 667–678. doi:[10.1088/0266-5611/9/6/005](https://doi.org/10.1088/0266-5611/9/6/005) E6
- [22] H. Harbrecht and T. Hohage, Fast methods for three-dimensional inverse obstacle scattering problems, *J. Integral Equations Appl.*, 19 (2007), pp. 237–260. doi:[10.1216/jiea/1190905486](https://doi.org/10.1216/jiea/1190905486) E6, E33
- [23] R. F. Harrington, Boundary integral formulations for homogeneous materials bodies, *J. Electromagnetics Waves and Applications*, 3 (1989), pp. 1–15. doi:[10.1163/156939389X00016](https://doi.org/10.1163/156939389X00016) E4
- [24] F. Hettlich, Fréchet derivatives in inverse obstacle scattering, *Inverse Problems*, 11 (1995), pp. 371–382. doi:[10.1088/0266-5611/11/2/007](https://doi.org/10.1088/0266-5611/11/2/007) E6
- [25] F. Hettlich, Erratum: “Fréchet derivatives in inverse obstacle scattering” [Inverse Problems **11** (1995), no. 2, 371–382; MR1324650 (95k:35217)],

- Inverse Problems*, 14 (1998), pp. 209–210.
doi:[10.1088/0266-5611/14/1/017](https://doi.org/10.1088/0266-5611/14/1/017) [E6](#)
- [26] F. Hettlich, The domain derivative of time-harmonic electromagnetic waves at interfaces, *Math. Methods Appl. Sci.*, 35 (2012), pp. 1681–1689.
doi:[10.1002/mma.2548](https://doi.org/10.1002/mma.2548) [E6](#), [E28](#)
- [27] T. Hohage, Logarithmic convergence rates of the iteratively regularized Gauss–Newton method for an inverse potential and an inverse scattering problem, *Inverse Problems*, 13 (1997), pp. 1279–1299.
doi:[10.1088/0266-5611/13/5/012](https://doi.org/10.1088/0266-5611/13/5/012) [E6](#), [E25](#), [E43](#)
- [28] T. Hohage, *Iterative Methods in Inverse Obstacle Scattering: Regularization Theory of Linear and Nonlinear Exponentially Ill-Posed Problems*, PhD thesis, University of Linz, 1999. [E6](#), [E25](#), [E26](#), [E43](#)
- [29] T. Hohage and C. Schormann, A Newton-type method for a transmission problem in inverse scattering, *Inverse Problems*, 14 (1998), pp. 1207–1227. doi:[10.1088/0266-5611/14/5/008](https://doi.org/10.1088/0266-5611/14/5/008) [E6](#)
- [30] O. Ivanyshyn and R. Kress, Identification of sound-soft 3D obstacles from phaseless data, *Inverse Probl. Imaging*, 4 (2010), pp. 131–149.
doi:[10.3934/ipi.2010.4.131](https://doi.org/10.3934/ipi.2010.4.131) [E43](#)
- [31] O. Ivanyshyn Yaman and F. Le Louër, Material derivatives of boundary integral operators in electromagnetism and application to inverse scattering problems, *Inverse Problems*, 32 (2016), pp. 095003, 24.
doi:[10.1088/0266-5611/32/9/095003](https://doi.org/10.1088/0266-5611/32/9/095003) [E40](#)
- [32] A. Kirsch, The domain derivative and two applications in inverse scattering theory, *Inverse Problems*, 9 (1993), pp. 81–96.
doi:[10.1088/0266-5611/9/1/005](https://doi.org/10.1088/0266-5611/9/1/005) [E6](#)
- [33] R. E. Kleinman and P. A. Martin, On single integral equations for the transmission problem of acoustics, *SIAM J. Appl. Math.*, 48 (1988), pp. 307–325. doi:[10.1137/0148016](https://doi.org/10.1137/0148016) [E5](#)

- [34] R. Kress, *Electromagnetic waves scattering : Scattering by obstacles*, Scattering, (2001), pp. 191–210. Pike, E. R. and Sabatier, P. C., eds., Academic Press, London. E6
- [35] R. Kress and L. Päivärinta, On the far-field in obstacle scattering, *SIAM J. Appl. Math.*, 59 (1999), pp. 1413–1426 (electronic). doi:10.1137/S0036139997332257 E6
- [36] F. Le Louër, *Optimisation de formes d’antennes lentilles intégrées aux ondes millimétrique*, PhDthesis, Univ. Rennes 1, 2009. <http://tel.archives-ouvertes.fr/tel-00421863/fr/>. E5, E6
- [37] F. Le Louër, A high order spectral algorithm for elastic obstacle scattering in three dimensions, *J. Comput. Phys.*, 279 (2014), pp. 1–17. doi:10.1016/j.jcp.2014.08.047 E7
- [38] F. Le Louër, Spectrally accurate numerical solution of hypersingular boundary integral equations for three-dimensional electromagnetic wave scattering problems, *J. Comput. Phys.*, 275 (2014), pp. 662–666. doi:10.1016/j.jcp.2014.07.022 E7
- [39] D. W. Mackowski, Analysis of radiative scattering for multiple sphere configurations, *Proc. Roy. Soc. London Ser. A*, 433 (1991), pp. 599–614. doi:10.1098/rspa.1991.0066 E22
- [40] P. A. Martin and P. Ola, Boundary integral equations for the scattering of electromagnetic waves by a homogeneous dielectric obstacle, *Proc. Roy. Soc. Edinburgh Sect. A*, 123 (1993), pp. 185–208. doi:10.1017/S0308210500021296 E4, E12, E13
- [41] J. R. Mautz, A stable integral equation for electromagnetic scattering from homogeneous dielectric bodies, *IEEE Trans. Antennas and Propagation*, 37 (1989), pp. 1070–1071. doi: 10.1109/8.34145 E4
- [42] C. Müller, *Foundations of the Mathematical Theory of Electromagnetic Waves*, Berlin-Springer, 1969. E4, E10

- [43] J.-C. Nédélec, *Acoustic and electromagnetic equations*, vol. 144 of Applied Mathematical Sciences, Springer-Verlag, New York, 2001. Integral representations for harmonic problems. [E9](#), [E40](#), [E42](#)
- [44] S. Onaka, Simple equations giving shapes of various convex polyhedra: The regular polyhedra and polyhedra composed of crystallographically low-index planes, *Philosophical Magazine Letters*, 86 (2006), pp. 175–183. doi:[10.1080/09500830600603050](#) [E23](#)
- [45] R. Potthast, Fréchet differentiability of boundary integral operators in inverse acoustic scattering, *Inverse Problems*, 10 (1994), pp. 431–447. doi:[10.1088/0266-5611/10/2/016](#) [E6](#)
- [46] R. Potthast, Domain derivatives in electromagnetic scattering, *Math. Methods Appl. Sci.*, 19 (1996), pp. 1157–1175. [E6](#)
- [47] R. Potthast, Fréchet differentiability of the solution to the acoustic Neumann scattering problem with respect to the domain, *J. Inverse Ill-Posed Probl.*, 4 (1996), pp. 67–84. doi:[10.1515/jiip.1996.4.1.67](#) [E6](#)
- [48] R. Song, X. Ye, and X. Chen, Reconstruction of scatterers with four different boundary conditions by T-matrix method, *Inverse Probl. Sci. Eng.*, 23 (2015), pp. 601–616. doi:[10.1080/17415977.2014.923418](#) [E40](#)

Author address

1. **Frédérique Le Louër**, Sorbonne Université, Université de technologie de Compiègne, LMAC EA2222 Laboratoire de Mathématiques Appliquées de Compiègne - CS 60 319 - 60 203 Compiègne cedex, France
<mailto:frederique.le-louer@utc.fr>
orcid:[0000-0002-6392-4281](#)